NWC TP 5330

AD-746133

(NASA-CR-127722) BERYLLIUM PARTICLE
COMBUSTION Final Report J.L. Prentice
(Naval Weapons Center) Jun. 1972 82 p
CSCL 21B
N72-28925
Unclas
G3/33 36011

Beryllium Particle Combustion
(Final Report)

by

Jack L. Prentice
Research Department

Naval Weapons Center
CHINA LAKE, CALIFORNIA ■ JUNE 1972

Approved for public release; distribution unlimited.

ABSTRACT

This report summarizes a two year study of the combustion efficiency of single beryllium droplets burning in a variety of oxidizers, but primarily mixtures of oxygen/argon and oxygen/nitrogen. An advanced laser heating technique has been used to acquire systematic quantitative data on the burning of single beryllium droplets at atmospheric pressure. This research confirms the sensitivity of beryllium droplet combustion to the chemistry of environmental species and provides experimental documentation for the nitrogen-induced droplet fragmentation of burning beryllium droplets. These studies clearly reveal the inadequacies of current droplet burning models as applied to beryllium but they also provide the sort of detailed, systematic foundation necessary for future rational development of the theory.

NWC Technical Publication 5330

Published by ....Research Department
Collation ....Cover, 32 leaves, DD Form 1473, abstract cards
First Printing ....195 unnumbered copies
Security classification ...........................UNCLASSIFIED

Naval Weapons Center
AN ACTIVITY OF THE NAVAL MATERIAL COMMAND
W. J. Moran, RADM, USN . . . . Commander
H. G. Wilson . . . . Technical Director

FOREWORD

This is the final report on a study of beryllium particle combustion efficiency sponsored by the National Aeronautics and Space Administration under Work Order 8201. The report covers the period 1 January 1969 to 31 December 1971. This program has been carried out in the Aerothermochemistry Division of the Research Department under the direction of Mr. Jack L. Prentice as Principal Investigator.

Limited subignition and particle agglomeration studies were conducted by Dr. K. J. Kraeutle as an adjunct to the particle combustion program and the results are described in an appendix to this report.

This report is transmitted for information only. It does not represent the official view or the final judgement of the Naval Weapons Center.

Released by
E. W. PRICE, *Head*
Aerothermochemistry Division
15 May 1972

Under authority of
HUGH W. HUNTER, *Head*
Research Department

CONTENTS

ACKNOWLEDGMENT

It is a pleasure to acknowledge illuminating discussions of this research with Drs. H. S. Levine, R. T. Meyer, and L. S. Nelson of the Sandia Laboratories, Albuquerque, New Mexico, during the preparation of this manuscript.

1. INTRODUCTION

This is the final report on a study of beryllium particle combustion efficiency. This study was the culmination of a long-range program of metal particle combustion research sponsored by the National Aeronautics and Space Administration (NASA) at the Naval Weapons Center (NWC). The initial focus of the research efforts at NWC was on aluminum particle combustion. Our investigations spanned a period of nine years during which significant advances in both experimental technique and fundamental knowledge of high temperature chemical processes were made. References 1-20 describe results of the research conducted in this laboratory during the period of NASA contract.

Metals are added to solid rocket propellants to increase their energy and density. Of the common candidate metals (aluminum (Al), beryllium (Be), magnesium (Mg), titanium (Ti), and zirconium (Zr)), Be has a specific heat of oxidation greater than all the others and twice as great as the more commonly used Al. The thermochemistry of Be has made it a desirable candidate on theoretical grounds but difficulties deriving from toxicity of its combustion products have inhibited its widespread use. Beryllium is still a relatively exotic material and its properties and combustion behavior have not yet been thoroughly explored nor completely characterized.

Prior to this study published accounts of Be particle combustion were very scarce and the theory was not well advanced. The current model of metal droplet burning still has critical inadequacies but this study has provided much of the needed data for further rational development of the theory.

The research conducted under this contract constitutes the most systematic quantitative Be particle combustion study available in this country. In view of the uncertain future of berylliumized propellants and the possible revival of interest the experimental data generated in this study are incorporated as appendixes to this report. It is hoped that, should a resurgence of interest occur, the availability of these data will preclude the re-plowing of much experimental ground. Because of a near-total lack of published results, a brief description of limited results from an adjunct study of Be particle agglomeration by Dr. K. J. Kraeutle is included as an additional appendix.

This report describes single particle Be combustion studies in which a pulsed neodymium-glass (Nd) laser (1.06 μ) was used as a remote ignition source. In this study systematic quantitative particle burning data were measured as functions of the oxygen mole fraction and original droplet diameter for various mixtures of oxygen-argon (O_2/Ar) and oxygen-nitrogen (O_2/N_2) at atmospheric pressure (700 ±7 torr).

2. EXPERIMENTAL METHODS

2.1. LASER IGNITION TECHNIQUE

Any technique used in the study of the combustion of metal particles which enables one to separate the ignition source from the oxidizing gases is a definite advantage. Laser ignition accomplishes this feat admirably. The laser ignition technique in use in this laboratory is one pioneered in the laboratory of L. S. Nelson of Sandia, and its development and application are described in detail in Ref. 10. The experiments are performed using a pulsed infrared laser operating at 1.06 μ with a nominal output of 15 joules in a 1 msec pulse. These experiments typically use 1.5-3.0 joules as ignition energy. With this improved pulse-heating apparatus, the light emitted by the burning metal particles may be used to record high speed motion pictures, still plate particle trajectories, photomultiplier intensity-time plots of particle radiation, and time-resolved emission spectra over the entire period from ignition to burnout. This technique has the important advantage over xenon flash heating that the ignition and the first few tens of milliseconds are not obliterated by radiation from the flash. Precise quantitative burning data are thus assured over a wide range of the experimental conditions which include the ability to vary pressure and composition of species in the environment as well as particle size.

2.2. MICROSCOPY

Microscopy is relied upon heavily as a diagnostic tool. Both conventional optical and scanning electron microscopes (SEM) are employed. Details of burnt particle geometry impossible to perceive by previously used techniques have been discovered by SEM and have contributed to significant advances in our understanding of metal particle combustion mechanisms. Application of the SEM to this type of combustion problem is detailed more fully in Ref. 14 and 15.

Combustion of Be in dry, nonhalogen oxidizers yields a large beryllium oxide (BeO) sphere as a major product. Measurement of the diameter of product spheres to an accuracy of ±1 μm with a Vickers[1] split-image measuring eyepiece yields information on the extent of metal loss from the parent droplet.

---

[1] Vickers Instruments, Inc., 15 Waite Court, Malden, Mass.

2.3 MATERIALS

Tank oxygen (aviator's breathing, 99.5%) and water-pumped Ar or N_2 were mixed as required for these experiments in a gas blender. All mixtures were passed through a drying train containing silica gel and molecular sieve immediately prior to use.

The Be used in these experiments (QV grade, 99.8%) was obtained from the Brush Beryllium Corp. and was in the form of foils 12.7 μm thick. These foils were cut into discs of various diameters in a miniature precision punch-press fabricated for the purpose. By changing punch sizes, discs were produced whose room temperature volume-equivalents corresponded to particles having diameters ranging from 221-392 μm.

A typical experiment is described briefly below. A very small Be disc (0.0127 mm thick by 0.635-1.524 mm diameter) is placed at the intersection of a set of fine cross-wires (0.038 mm Al) which are supported on a C-shaped metal holder. The specimen holder is housed in a rectangular heavy-wall stainless steel reaction vessel which has Pyrex windows on the front and back. The sample holder is articulated by means of a 3-axis manipulator operating through a stainless steel bellows attached to the reactor wall. A Be disc is placed on the cross-hairs and positioned at the laser focus, the atmosphere in the vessel adjusted to the desired composition and pressure, and the laser fired remotely to ignite the particle. The droplet burns in free-fall and characteristic burning parameters are measured photographically and photometrically. Droplet radiation is measured with an RCA 7102 photomultiplier viewing the combustion through a narrow band-pass filter with peak transmission at 8100 ±50 Å. Burning times are measured from oscilloscope records of the photomultiplier intensity-time trace. Still plate track photographs of the burning droplet are made simultaneously.

2.4. X-RAY STUDIES

As part of the study aimed at the X-ray characterization of the reaction intermediates, various mixtures of reagent grade BeO and Be_3N_2 were fused in atmospheric air by radiation from a 200 watt CO_2 laser and submitted for powder diffraction analysis.

3. SINGLE PARTICLE COMBUSTION

The limited quantitative Be particle burning data available prior to this study came from powder-burning torch-flame experiments. The considerable scatter in such data arises mainly from uncertainties in ignition delay times, flame temperature and composition, and particle size. Such experiments employ powder screen fractions and as a result the uncertainty in the particle size may be as great as ±20%. Whereas the uncertainty in burning data from those previous techniques was as great as a factor of two, these laser experiments yield burning data with a scatter typically of ±7% or less. Precise control of disc sizing yields particles whose diameters are known to ±1.5%. A photograph of the apparatus may be seen in Fig. 1.

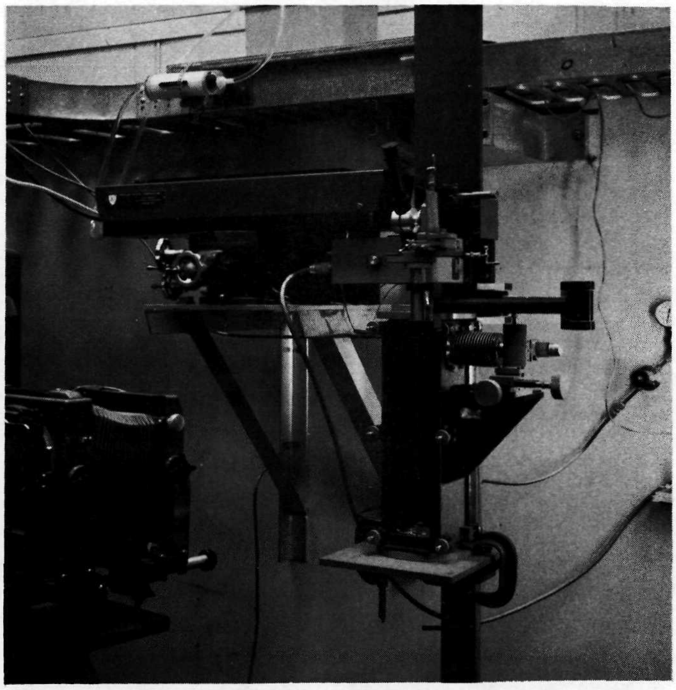

FIG. 1. Apparatus for Single Particle Laser Ignition Studies.

3.1. BURNING IN OXYGEN/ARGON

Characteristic droplet burning times have been measured from photomultiplier intensity-time plots as functions of both droplet size and O_2 mole fraction for various mixtures of O_2 in Ar. As mentioned earlier, a major combustion product of the burning of Be in O_2/Ar mixtures is a large sphere of BeO. The diameter of the resultant sphere is also routinely measured on each particle burned.

Beryllium and Al are said to burn by a "vapor transport" process; that is, the reaction occurs preponderantly by transport of metal vapor to the region surrounding the droplet where it reacts with oxidizer(s) at some stand-off distance to form the stoichiometric oxide. This reaction scheme is a hydrocarbon droplet combustion analogy and, as such, amounts to a considerable over-simplification. As its greatest shortcoming it fails to adequately treat the back-diffusion and accumulation of oxide on the droplet surface. In the case of Al this results in a discrete globule of oxide on the droplet producing marked asymmetry but not total encapsulation. In the case of Be the oxide completely encapsulates the droplet during burning and as a consequence exerts a proportionately greater effect on the combustion. The reasons for such behavior will become clear later in the discussion.

A schematic history of the emission from a typical Be particle burning in O_2/Ar may be seen in Fig. 2. Good correlation of the photomultiplier record is found with the still plate track photograph in Fig. 3, where the "bloom" on the track corresponds to the region of maximum vapor phase reaction and the spearpoint identified the time of onset of freezing of the encapsulating BeO. This "spearpointing" is indicative of supercooling and subsequent freezing of an oxide coating on the particle.

As the particle track shows, the combustion dynamics are somewhat more complicated than was previously supposed. Previously published track photographs do not indicate such blooming (Ref. 17 and 21) and the spearpoint associated with supercooling and freezing of the oxide has not previously been reported in Be combustion. Such spearpointing is characteristic of Ti and Zr (Ref. 11 and 22). Rapid oscillation of the photomultiplier trace in Fig. 2 shows that the particle spins vigorously from ignition to onset of freezing of the surface BeO. Track photographs

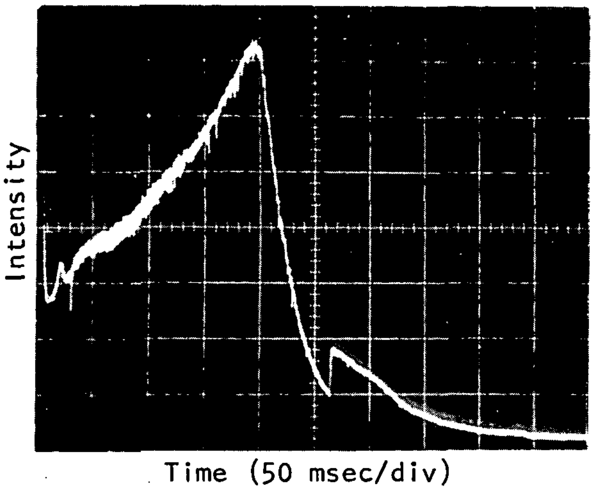

FIG. 2. Oscilloscope Record of Photomultiplier Intensity-Time Trace of 326 μ Be Droplet Burning in 50/50 O_2/Ar at 700 ±7 Torr. Note evidence of particle spin up till onset of freezing. Discontinuity at 260 msec represents supercooling and spearpointing associated with freezing of surface oxide.

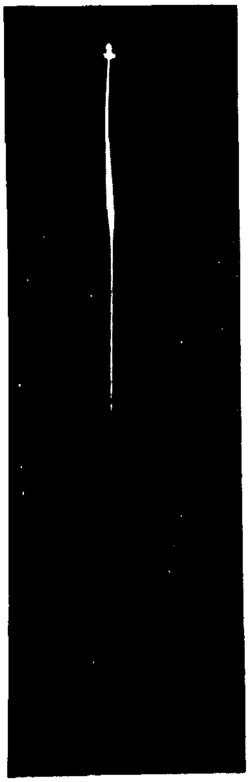

FIG. 3. Time-exposed Track Photograph of a 326 μ Be Droplet Burning in 50/50 O_2/Ar at 700 ±7 Torr.

of xenon flash-ignited Be particles appeared to be devoid of character due to the early phases of the combustion being obscured by flashlamp radiation as well as physically obscured by portions of the apparatus. Details of the burning mechanism inferred from quenching studies performed as part of the earlier flash ignition experiments are, however, validated by these more recent laser ignition studies.

Previous studies of flash-heated Be particle combustion reported from this laboratory (Ref. 16 and 17) showed that ignition can occur below the metal melting point accompanied by considerable smoke and rather massive growth of randomly oriented clusters of BeO needles. The rising particle temperature produces a molten Be droplet with a uniform growth of perfect hexagonal BeO whiskers; further rise in droplet temperature melts the BeO into a coherent coating which may become quite thick ($\sim$50 μm) before radiant heat loss overwhelms heat production resulting in freezing of the oxide.

All investigators have found that burning Be droplets, while exhibiting strong vapor phase reaction, are accumulating oxide simultaneously. The evidence from this study indicates that vapor phase and surface reaction are concurrent. Growth of the BeO whiskers early in burning does not seem to be a simple condensation phenomenon. Attention has already been directed to the fact that a sphere of BeO remains following termination of combustion. Figure 4 shows that the diameter of this sphere increases linearly with increase in O_2 mole fraction. Plotting the ratio of final to initial particle size (μ_f/μ_o) versus O_2 mole fraction as in Fig. 5 shows that the final BeO sphere size equals the original Be droplet size when the O_2 mole fraction is approximately 0.55-0.7. At all O_2 mole fractions greater than about 0.7 the final sphere size is greater than the original Be droplet size. In Fig. 6 the data of Fig. 5 are replotted to show the weight fraction of Be lost (vaporized) from the droplet as a function of O_2 mole fraction. This figure shows that more metal is lost at low O_2 mole fraction than is lost at high O_2 mole fraction. This seeming paradox occurs because of the following circumstances.

In general, BeO accumulates on the droplet surface forming an increasingly impermeable barrier to metal vapor efflux until the detached flame collapses onto the droplet surface. Complete encapsulation of the droplet occurs sooner in high O_2 concentration. The strongly radiating oxide surface is cooling the droplet even further and shortly the surface BeO freezes. The onset of freezing tends to further slow the reaction. It is important to note, however, that BeO freezes at a temperature about 60° higher than the metal boiling point. The very high residual droplet temperature coupled with the presence of numerous large cracks in the oxide crust ensure that reaction, though diminished, may proceed. It is known from previous quenching studies associated with the flash heating experiments (Ref. 17) that considerable metal remains in the particle at the onset of freezing and that smoke is absent shortly thereafter. The experiments reported here show that the completely burnt and

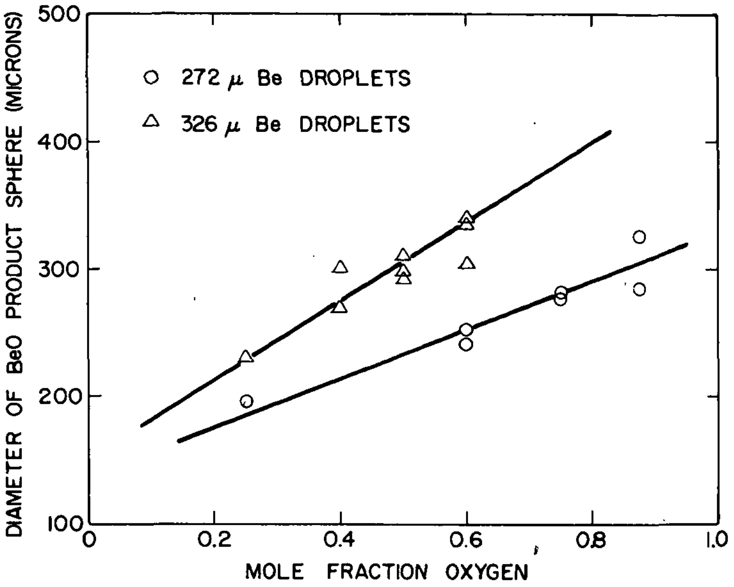

FIG. 4. Variation of Size of BeO Product Sphere With O_2 Mole Fraction for a Series of Original Be Droplet Sizes Burning in O_2/Ar Mixtures at 700 ±7 Torr.

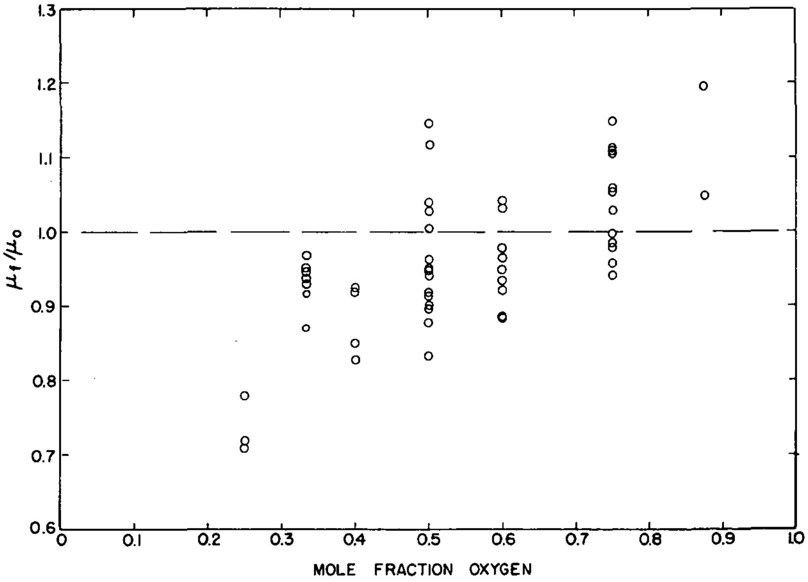

FIG. 5. Variation of the Ratio of Final to Initial Particle Size (BeO/Be) as a Function of O_2 Mole Fraction for a Series of Be Droplets Burning in O_2/Ar at 700 ±7 Torr.

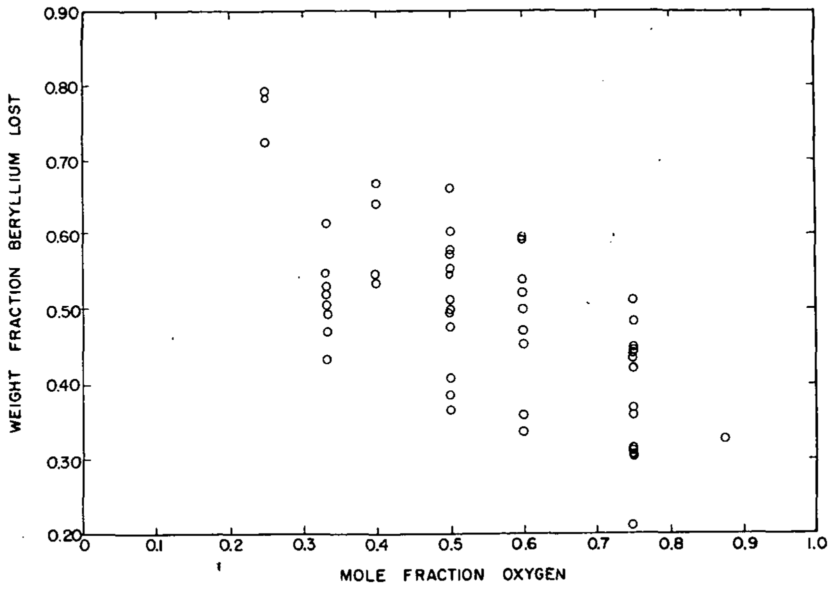

FIG. 6. Calculations From Data in Fig. 4 Plotted to Show the Weight Fraction of Be Lost From the Parent Particle as a Function of O_2 Mole Fraction for Be Droplets Burned in O_2/Ar at 700 ±7 Torr.

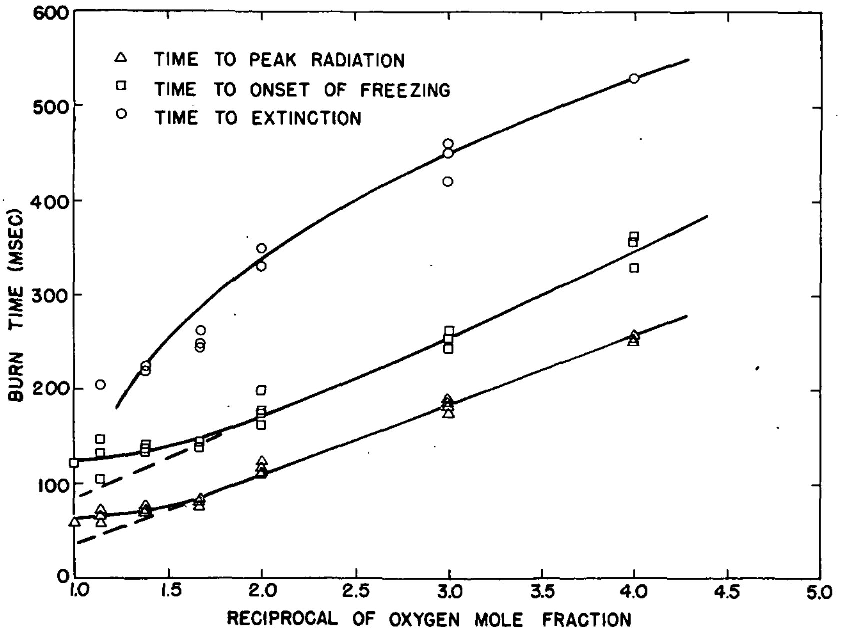

FIG. 7. Plot of the Characteristic Burning Times Versus the Reciprocal of O_2 Mole Fraction for 272 µ Be Droplets Burning in O_2/Ar at 700 ±7 Torr.

extinguished BeO sphere has neither remaining metal nor voids. We therefore believe that no further metal is lost from the droplet following freezing and that the metal remaining at the time of freezing must react by a slower surface mechanism.

These studies and the work of others have shown both vapor phase and surface types of reaction mechanism to be possible. To say that one or the other occurs exclusively would seem to place too restrictive an interpretation on the experimental facts. The vapor phase model of metal burning is a diffusion-limited model, i.e., the burning rate is limited by gas-phase diffusion of the oxidizer. Such a theory predicts that the droplet burning time should be inversely proportional to the O_2 concentration. Figure 7 shows the characteristic burning times for 272 μm Be particles plotted versus the reciprocal of O_2 mole fraction. It is seen that the time to peak radiation (assumed to correspond to time of maximum reaction) and the time to onset of freezing of oxide are indeed proportional to reciprocal O_2 mole fraction up to an O_2 concentration of about 60%. In the neighborhood of 55-60% O_2 both curves depart from their former slope. The time to extinction of the droplet appears to show no direct proportionality.

A plot of this type would not seem to be able to distinguish between vapor phase and condensed phase reaction since both processes are diffusion-limited. It would not seem to certify the existence of one to the exclusion of the other. Rather, it appears that the change in slope exhibited by the two curves above $X_{O_2} = 0.6$ is indicative of a transition from vapor phase ($X_{O_2} \leq 0.6$) to condensed phase ($X_{O_2} \geq 0.6$)as the controlling mechanism. In support of this contention note that Fig. 6 shows less than 50% metal lost for all $X_{O_2} > 0.6$. The point should be made here that we do not believe that either process ever occurs to the exclusion of the other. We suggest that one or the other process is dominant in a given regime of O_2 concentration and that the plot in Fig. 7 shows the region of transition in dominant mechanism.

To go one step further, there are actually three distinct reaction regimes, if not to say mechanisms, occurring during the burning history of a single Be particle. At virtually all O_2 concentrations the following reaction sequence seems to obtain following ignition:

1. Predominantly vapor phase prior to encapsulation
2. Predominantly condensed phase reaction through molten oxide following encapsulation
3. Predominantly condensed phase reaction through solid oxide crust as terminal stage.

This sequence is likely to be modified for Be droplets burning in rocket motors or torch flames if the flame-generated ambient temperature is greater than 2820°K. In that case only conditions (1) and (2) obtain.

Data on the burning time of these Be droplets as a function of particle diameter are given in Fig. 8 and 9. The data are still of a preliminary nature and more experiments are needed but they do show a direct proportionality between the time to burnout or extinction and particle size. Figure 8 shows all three characteristic burning times ($t_{\text{peak rad.}}$, t_{freeze} and t_{extinct}) for a series of particle sizes burned in 75% O_2/Ar mixtures. The greater scatter, relatively, in the extinction times is a result of trying to read the intersection of two asymptotic curves on the oscilloscope trace. Additionally, as long as an oxide clinker is the major product species the time to actual burnout will be difficult to specify with certainty since there will always be a small, but finite added time for thermal decay of the sphere to extinction.

3.2. SUMMARY OF BURNING IN OXYGEN/ARGON

These experiments provide much-needed data of sufficient precision to help evaluate current theoretical droplet burning models. While some of the data are still quite preliminary, they are adequate to permit discrimination. In agreement with Macek and Semple (Ref. 23), these experiments show that two or more distinct modes of combustion are possible. Our laser-ignition experiments show that the droplet burning time is proportional to the particle diameter, contrary to Macek and Semple. Those authors claim a d^2 dependence but their data appear too scanty to support the claim. Assuming a conventional burning rate relationship such as $t_{\text{burn}} = kd^n$ for these laser-ignited Be droplets a plot of log t_{burn} versus log diameter yields values of the exponent "n" ranging from 1.19 at an O_2 mole fraction of 0.33 to a value of 1.31 at an O_2 mole fraction of 0.75. Thus it is further demonstrated that the present idealized vapor phase model, when applied to Be, fails one of its fundamental tests.

Our experiments suggest a change in controlling mechanism from vapor phase to surface reaction at O_2 mole fractions above about 0.6. A large BeO sphere is a major product of reaction of Be droplets burning in O_2/Ar mixtures. The size of this sphere increases linearly with O_2 mole fraction and equals or exceeds original droplet diameter at O_2 mole fractions greater than about 0.55-0.7. Oxide on the droplet surface freezes during burning terminating further metal loss from the particle but not further reaction. The size of the BeO sphere is such that at O_2 mole fractions greater than 0.6 more than 50% of the metal is incorporated in the sphere at the completion of burning.

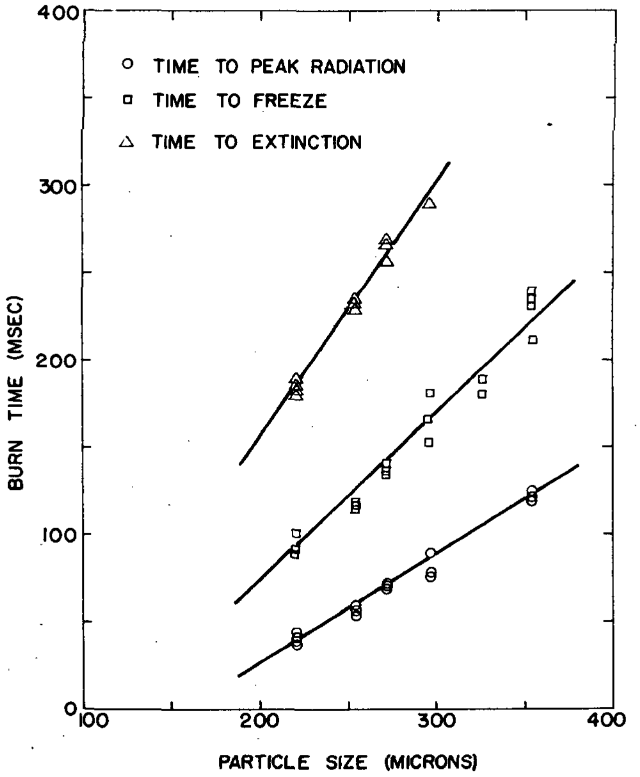

FIG. 8. Plot Showing Variation in Characteristic Droplet Burning Times as a Function of Particle Diameter for Be Droplets Burning in 75% O_2/Ar at 700 ±7 Torr.

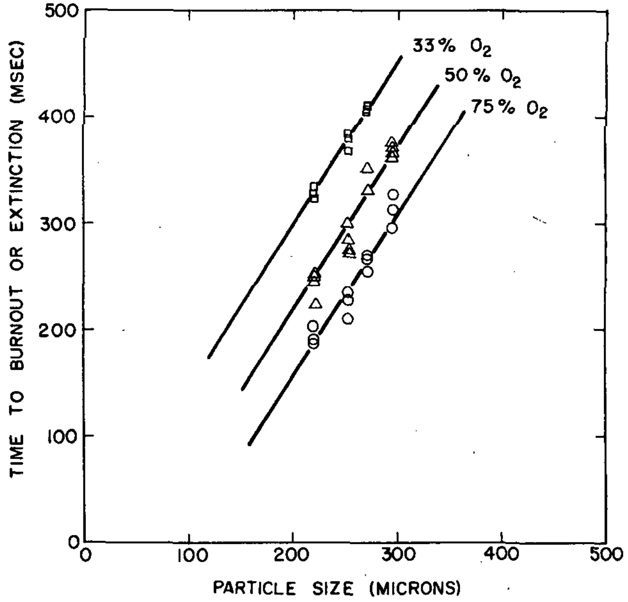

FIG. 9. Plot Showing the Variation in Time-to-Burnout or Extinction as a Function of Particle Size for a Series of Be Droplets Burned in Various O_2/Ar Mixtures at 700 ±7 Torr.

The theoretical treatments published to date yield results which do not correspond to the findings of these laser heating experiments. The treatment of Kuehl and Zwillenberg (Ref. 24), the most elaborate to date, errs in predicting no oxide accumulation on particles larger than 50 μm for $X_{O_2} \leq 0.4$. Their analysis predicts that the BeO spheres should not be larger than 0.6 times the original droplet diameter and it yields burning times too long by a factor of 2.5.

The experiments of Macek and Semple and our laser heating tests are not directly comparable because of vastly different particle sizes and ambient temperature. Trends with particle size should be comparable, however, although the effect of high ambient temperature in their experiments remains a significant factor more likely to produce differences in degree rather than in kind. Its greatest qualitative effect is likely to be with respect to its tendency to keep surface oxide molten.

There are many areas of agreement between the findings of Macek and Semple (Ref. 23) and our laser ignition experiments. Superficially, the droplet combustion appears the same: pronounced particle spin, strong vapor phase reaction with accretion of oxide on the droplet surface, and diffusely luminous tracks. Three modes of reaction are recognized in each investigation, but where each notes reduced diffuse luminosity, narrowed particle tracks and lowered color temperature for droplets burning in the presence of water vapor, the explanations differ. Macek and Semple propose that these phenomena are attributable to an exceptionally heavy preignition deposit of oxide on the particle which then keeps the vapor pressure of Be relatively low even after ignition. We have been able to show that, rather than produce a heavy oxide coat in water vapor, actually the reverse is true. Reaction of burning Be droplets with water vapor removes all oxide from the droplet surface, probably by the reaction:

$$BeO_{(s)} + H_2O_{(gas)} \rightleftharpoons Be(OH)_{2(gas)};\ \Delta H^\circ_{298} = +42 \text{ kcal/mole}$$

The endothermicity of this reaction is heat sink enough to reduce both color temperatures and diffuse luminosity and increase burn times by the 30% reported by Macek and Semple. No BeO spheres result from combustion in the presence of water vapor.

3.3. BURNING IN OXYGEN/NITROGEN

Nitrogen, considered by many to be inert, is known to be a reactant in numerous high temperature gas-metal systems (Ref. 25). Much confusion and some controversy arose in the early metal particle combustion literature because of less than widespread recognition of the fact that N_2 does indeed play an active role.

We intend to show in this report that Be also reacts with N_2 at droplet combustion temperatures and that the presence of N_2 causes bubble blowing and violent particle fragmentation in various mixtures of O_2/N_2.

Nitrogen is shown here to retard the ignition and all subsequent stages of combustion except fragmentation. The main impetus for Be combustion comes from rocket propellant applications, and solid rocket combustion products contain significant concentrations of N_2. Therefore, the effect of N_2 on burning Be droplets is of immediate practical importance.

Nitrogen has been known for some time to have a dramatic effect on the oxidation of Be at elevated (>500°C) temperatures (Ref. 26). With but few exceptions (Ref. 8, 27 and 28), little note has apparently been taken of the prospect of significant involvement of N_2 in metal droplet combustion processes. This oversight appears peculiar in view of the fact that the nitrides of most of the metals whose combustion has been studied appreciably have high negative free energies of formation at reasonable droplet temperatures (see Table I). Further, the metals are often burned in air with an overwhelming concentration of N_2. Magnesium, the only apparent contradiction in this series, has a droplet boiling temperature of 1378°K at which point the free energy of formation of the nitride is -44.7 kcal/mole, so the generalization is still valid.

TABLE 1. Free Energies of Formation of Some Selected Metal Nitrides.

	AlN	BN	Be_2N_3	TiN	ZrN	Mg_3N_2
ΔF°_{298}	-68.6	-60.0	-127.3	-73.8	-80.5	-95.8
ΔF°_{2500}	- 9.2	-64.7	- 26.3	-23.8	-30.9	+94.9

NOTE: From JANAF Thermochemical Tables, Dow Chemical Company, Midland, Michigan, 1965, plus Addenda.

In what follows below we shall describe the results of quantitative single particle combustion experiments which detail the effect of N_2 as a reactant in Be combustion. Experimental documentation of the fragmentation of Be droplets burning in the presence of N_2, first reported from this laboratory (Ref. 20), is elaborated in this report. The behavior of Be droplets burning in mixtures of O_2/N_2 is compared in detail with the above systematic data on the system $Be/O_2/Ar$.

The salient qualitative features of the combustion of Be droplets in both O_2/Ar and O_2/N_2 may be seen in Fig. 10. This figure compares the still-plate track photos and photomultiplier radiant emission histories of particles burned in both gas mixtures. As we have seen above, particles burned in O_2/Ar exhibit three characteristic burning times as measured from the photomultiplier oscilloscope record. These are: time to peak radiation, t_{pk}, assumed to correspond to time of max reaction; time to onset of freezing, t_{freeze}, which is indicative of the supercooling and subsequent freezing of the encapsulating surface oxide and

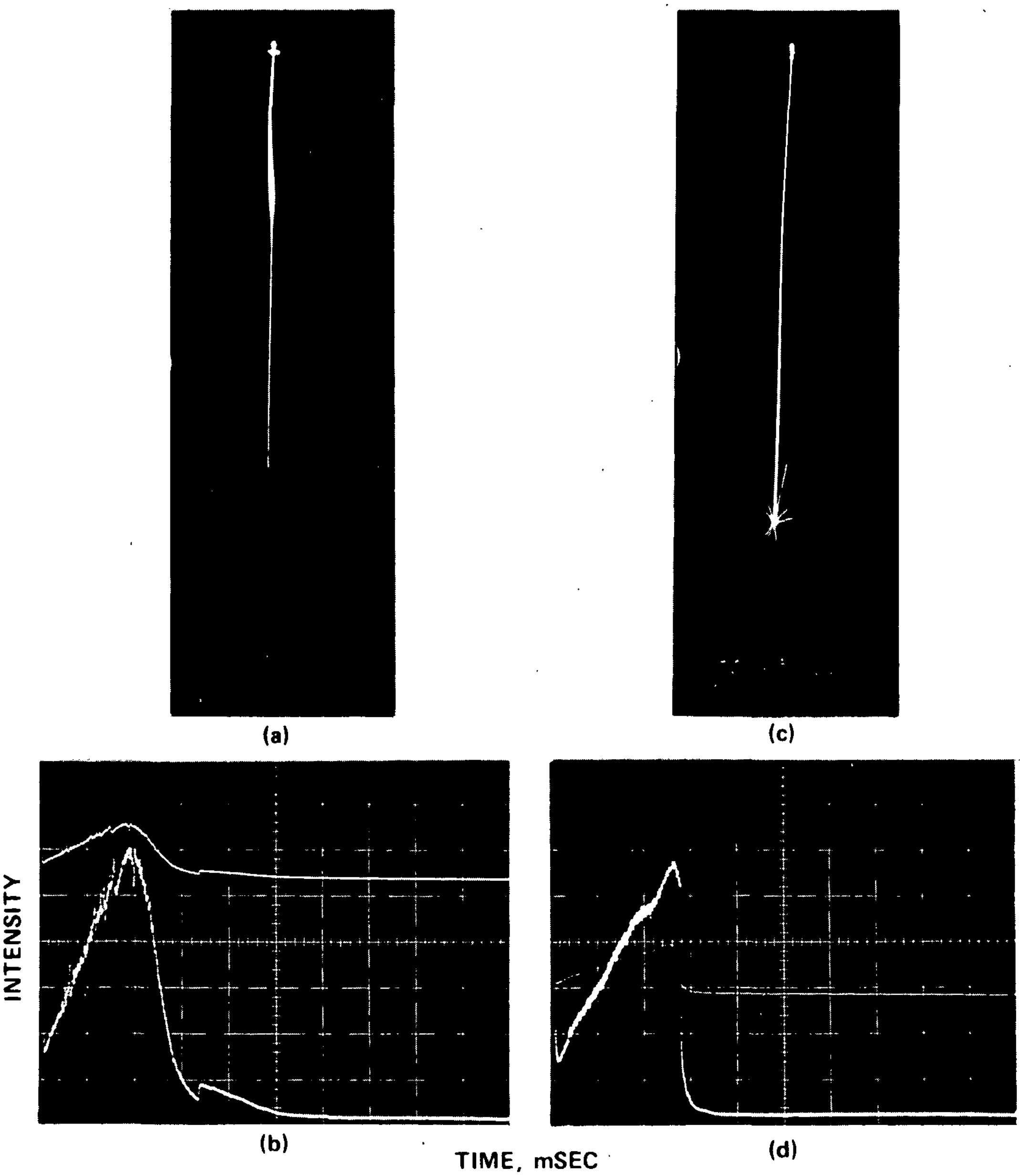

FIG. 10. Still Plate Track Photographs and Oscilloscope Trace of Photomultiplier Records for Laser-Ignited Be Particles Burning (a, b) in 50/50 O_2/Ar, and (c, d) in 50/50 O_2/N_2 at 700 ±7 Torr. Note particle explosion in O_2/N_2 and no explosion in O_2/Ar.

which may be correlated with the "spearpoint" on the track photo; and finally time to burnout or extinction, $t_{extinct}$, manifested by droplet radiation going to zero. Under these circumstances, the dominant reaction product is a large BeO sphere. Beryllium droplets burned in some O_2/N_2 mixtures are seen to explode violently as in Fig. 10c. Unlike the other metals whose combustion has been reported, Be has both lower and upper thresholds of N_2 concentration for droplet fragmentation. In addition, the droplets are found to blow balloons of oxide about 1.5 times original droplet diameter at both thresholds. Outside of the explosion limits the Be droplets burn qualitatively like those in O_2/Ar yielding similar photomultiplier records and again producing BeO spheres.

Figure 11 shows the fragmentation limits as well as the ignition limit for five particle sizes (221, 254, 272, 296, 326 µm) burning in mixtures of O_2/N_2. Complete data over the whole range of stoichiometry are given for four sizes, explosion data are given for all five sizes. In this figure the time-to-termination (either explosion or conventional burnout) for all particles burned is plotted as a function of O_2 mole fraction. With the exception of those specimens right on a threshold each point on the plot represents the mean of 3-6 replicate experiments. When burning at threshold conditions some particles will fragment and others will not. Those not fragmenting yield a BeO sphere and thus a conventional burnout or extinction measurement. Accordingly, the threshold behavior of the individuals in the group is displayed to indicate the dramatic difference in burn time between the two different cases. In all data plots which follow, unless specified otherwise, each data point represents the mean of 3-6 replicate experiments.

It can be seen that the droplet fragmentation times all cluster very tightly and almost exclusively between 40 and 60% O_2 in N_2. The only particle size which was found to fragment below 40% O_2 was the 221 µm group at 33% O_2. Even this condition is marginal, however, since less than half of the particles irradiated at this condition would ignite. It was found that the droplet explosions were both N_2-concentration and particle size-dependent. Not all particle sizes studied exploded at all gas compositions within the explosion limits. For example, the larger particles exploded more readily at high O_2 mole fraction while the smaller particles exploded more readily at lower O_2 mole fraction. As an aid to proper orientation on this plot the reader may consider the vertical string of five small black dots at O_2 mole fraction = 0.5. This string of data points (each the mean of five experiments) represents the time-to-fragmentation for five different particle sizes at 50% O_2/N_2, with t_{frag} 221 µm at the bottom and t_{frag} 326 µm at the top.

Table 2 summarizes the types of burning behavior for all the experiments in O_2/N_2. In cases where notations such as (Frag/SP) and (SP/Frag) appear it means this is a threshold condition with both types of behavior present with the first-mentioned occurring in the majority of cases.

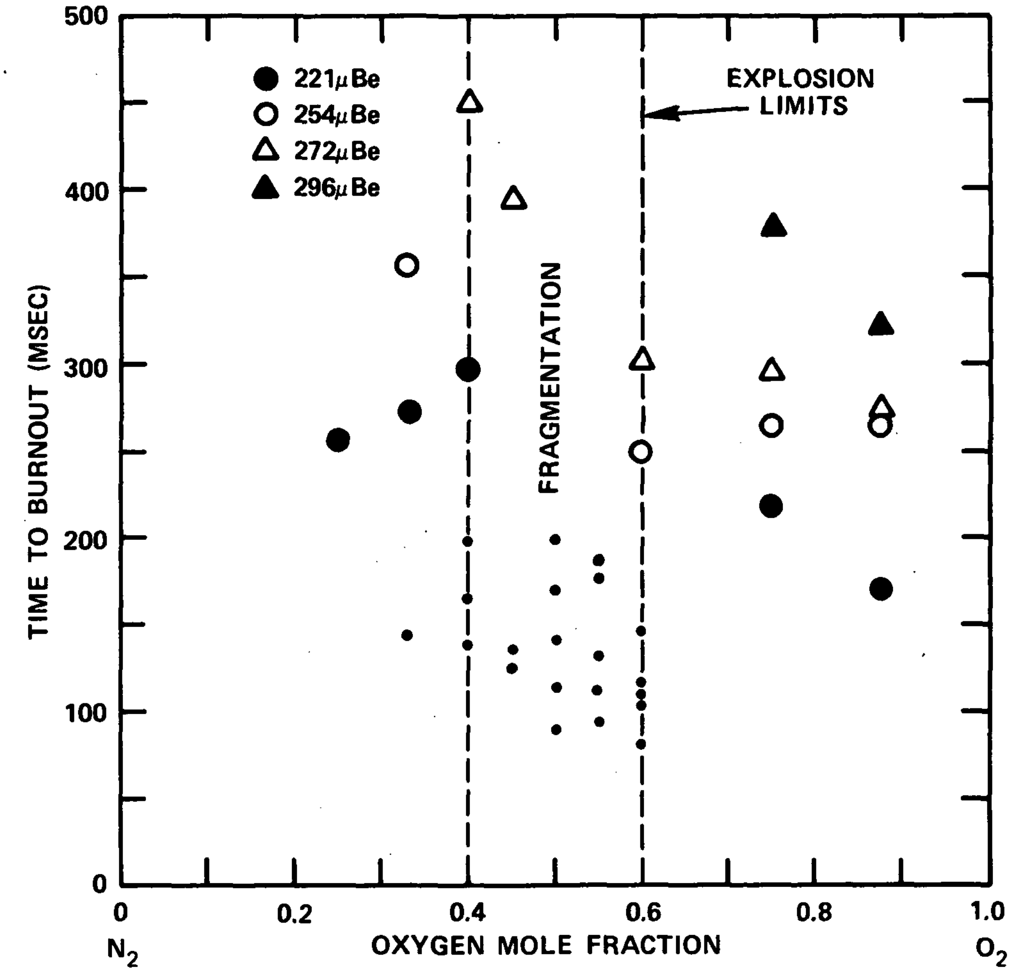

FIG. 11. Plot of Burnout or Fragmentation Time Versus O_2 Mole Fraction for Laser-Ignited Be Droplets Burning in O_2/N_2 Mixtures at 700 ±7 Torr. This plot shows that Be has both upper and lower thresholds of N_2 concentration for droplet explosion. Explosion limits are at 40 and 60% O_2 in N_2. Outside this concentration range particles burn like O_2/Ar (cf. Fig. 3).

Figure 11 shows that the ignition limit for this series of particle sizes is at an O_2 mole fraction of 0.25 at laboratory ambient temperature. Actually, the ignition limit itself is size dependent with only a few of the 221 μm particles igniting at 25% O_2. Figure 12 shows, in part, that for fixed particle size, the ignition limit is lower in O_2/Ar than in O_2/N_2, since 272 μm droplets ignite at an O_2 mole fraction as low as 0.25 in O_2/Ar while they won't ignite below 0.4 in O_2/N_2. Thus it is seen that the presence of N_2 inhibits the ignition of Be droplets. Figure 12 also shows that N_2 increases the time to attain maximum reaction.

TABLE 2. Summary of Burning Characteristics for Laser-Ignited Be Droplets Burning in Dry O_2/N_2.

Original particle diameter	Oxygen mole fraction								
μm	0.25	0.33	0.40	0.45	0.50	0.55	0.60	0.75	0.875
221	SP[a]	Frag[b]	Frag	Frag	Frag	Frag	SP/Frag	SP	SP
254	DNI[c]	SP	Frag	Frag	Frag	Frag	Frag	SP	SP
272	DNI	DNI	Frag/SP	Frag	Frag	Frag	Frag/SP	SP	SP
296	DNI	DNI	SP	SP	Frag	Frag	Frag	SP	SP
326	DNI	DNI	SP	...	Frag	Frag	Frag	...	...
354	DNI	DNI	...	...	...	...	Frag	...	...

[a] Spearpoint (i.e., it burns qualitatively like O_2/Ar).
[b] Fragmentation.
[c] Does not ignite.

As noted earlier, the presence of N_2 affects all stages of the combustion. The effect is not uniform, however, as can be seen by comparing Fig. 13, 14, and 15. In these figures the characteristic burning times (t_{pk}, t_{freeze}, $t_{extinct}$) are plotted as functions of the reciprocal of the O_2 mole fraction to emphasize the differences in behavior between Ar and N_2 and to more readily reveal any changes in mechanism which may occur. It is important to keep in mind during the examination of these three figures that 272 μm particles would not ignite below 40% O_2 in N_2. Figure 13 shows the time to peak radiation as a function of reciprocal O_2 mole fraction for Be droplets burning in both O_2/Ar and O_2/N_2. It can be seen that the presence of N_2 increases the time to peak radiation (max reaction) and, as might be expected, the effect is greater the greater the concentration of N_2. In Fig. 14, which shows t_{freeze} vs. reciprocal O_2 mole fraction, the difference between Ar and N_2 becomes dramatic. This plot shows the discontinuity in behavior associated with crossing the fragmentation zone. In Fig. 15, which shows $t_{extinct}$ vs. reciprocal O_2 mole fraction the discontinuity is much more pronounced and the slope of $t_{extinct}$ vs. $1/X_{O_2}$ changes radically in crossing the fragmentation zone.

Burning parameters were also measured as a function of original particle size (d_o). Figure 16 compares time to peak radiation versus particle size for both O_2/Ar and O_2/N_2 mixtures. Again the retarding effect of N_2 is evident. In Fig. 17 the same data are included to indicate where the particles fragment relative to the "normal" burning sequence in O_2/Ar. The figure demonstrates that for fixed particle size and fixed O_2 concentration, the Be droplets burning in O_2/N_2 will explode at times just prior to the normal freezing of the surface oxide.

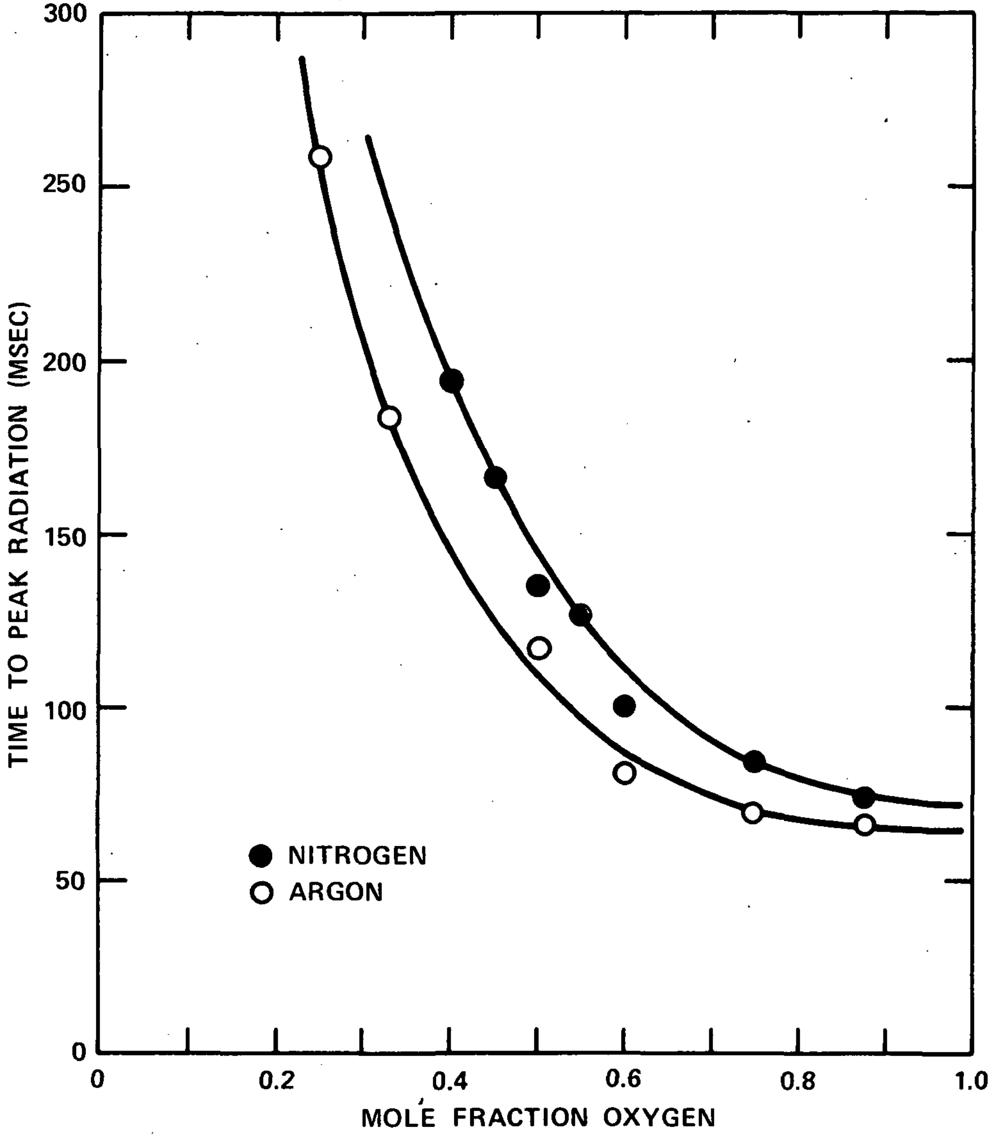

FIG. 12 . 272 μm Be Particles Burning in O_2/Ar and O_2/N_2 Mixtures at 700 ±7 Torr. Plot shows time to peak radiation (maximum reaction) as a function of O_2 mole fraction. Retarding effect of N_2 is obvious as well as the fact that ignition limit is lower in O_2/Ar than in O_2/N_2.

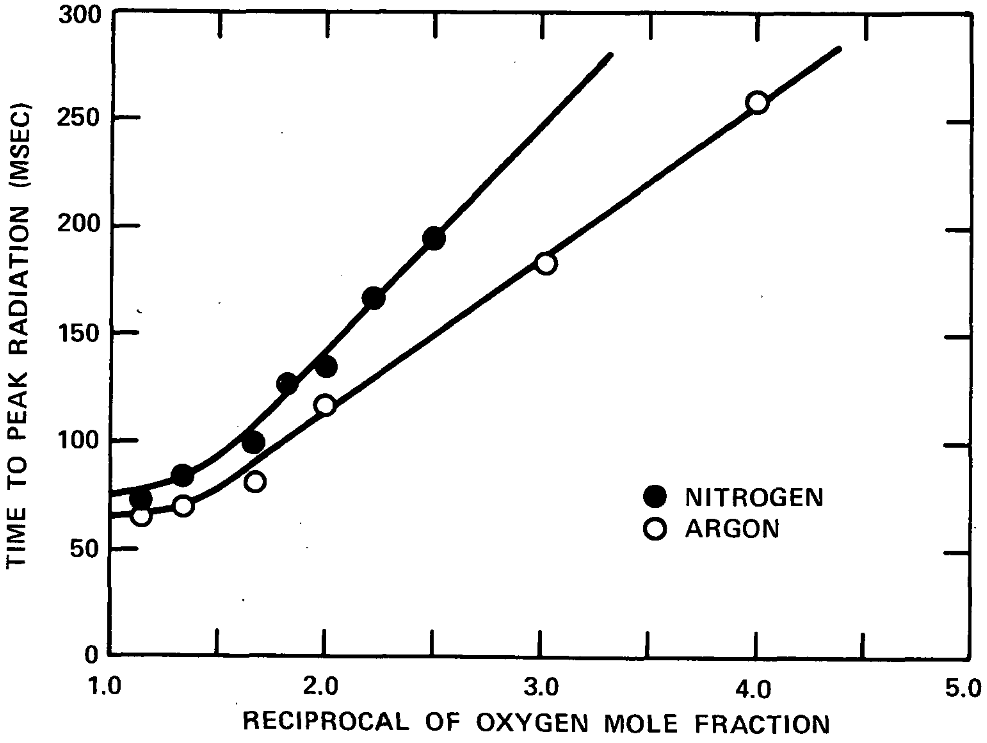

FIG. 13. 272 µm Be Droplets Burning in Mixtures of O_2/Ar and O_2/N_2 at 700 ±7 Torr. Plot of $t_{\text{peak radiation}}$(maximum reaction) versus reciprocal O_2 mole fraction showing change of controlling mechanism at about 60% O_2. No ignition below 40% O_2 in N_2.

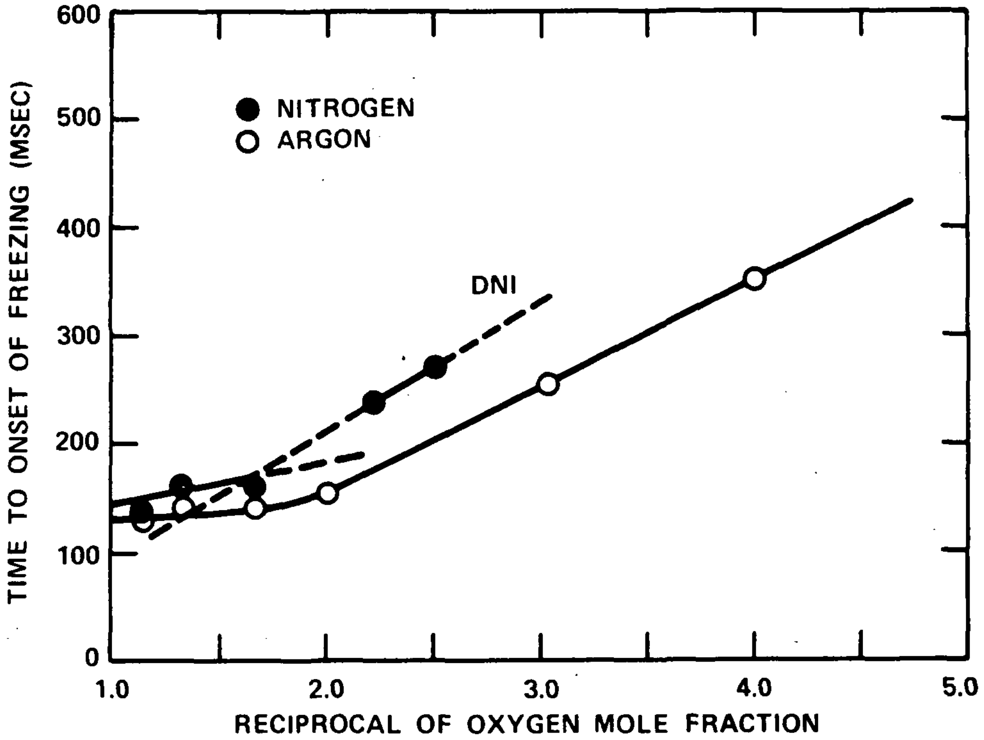

FIG. 14. 272 µm Be Droplets Burned in O_2/Ar and O_2/N_2 Mixtures at 700 ±7 Torr. Plot of time to onset of freezing of surface oxide versus reciprocal O_2 mole fraction. No particles freeze between 40 and 60% O_2 (explosion). Note retarding effect of N_2 on reaction rate and significant change of slope of N_2 curve in crossing explosion zone. (DNI = does not ignite.)

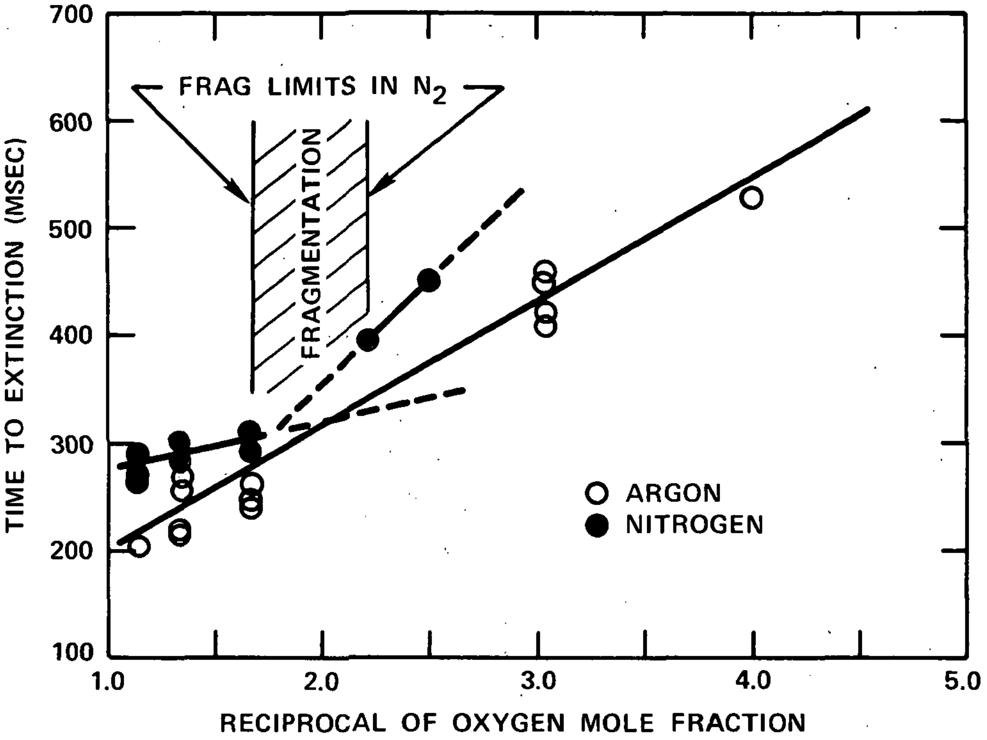

FIG. 15. 272 µm Be Droplets Burned in Mixtures of O_2/Ar and O_2/N_2 at 700 ±7 Torr. Plot shows time to extinction versus reciprocal O_2 mole fraction. Retarding effect of N_2 on reaction is apparent. Note dramatic change of slope in N_2 curve when crossing explosion zone.

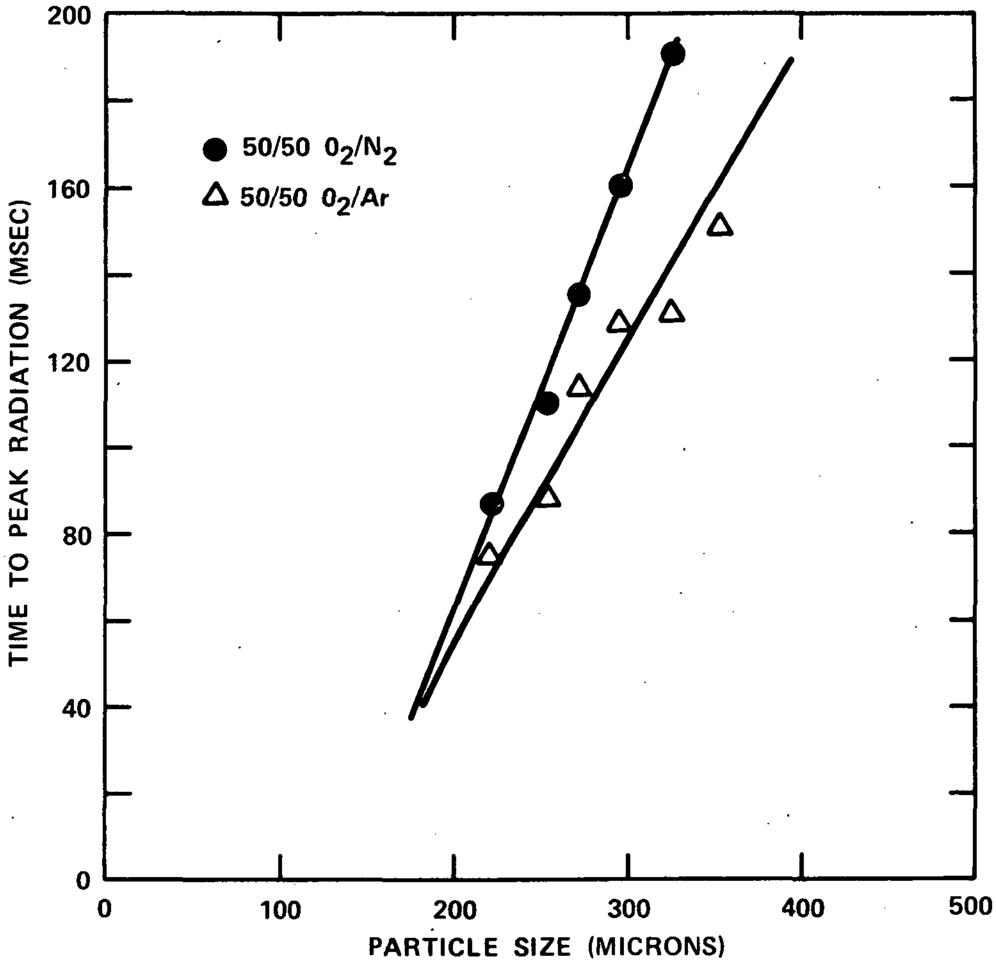

FIG. 16. Time to Peak Radiation (Maximum Reaction) Versus Original Droplet Diameter for Be Droplets Burning in 50/50 Mixtures of O_2/Ar and O_2/N_2 at 700 ± Torr.

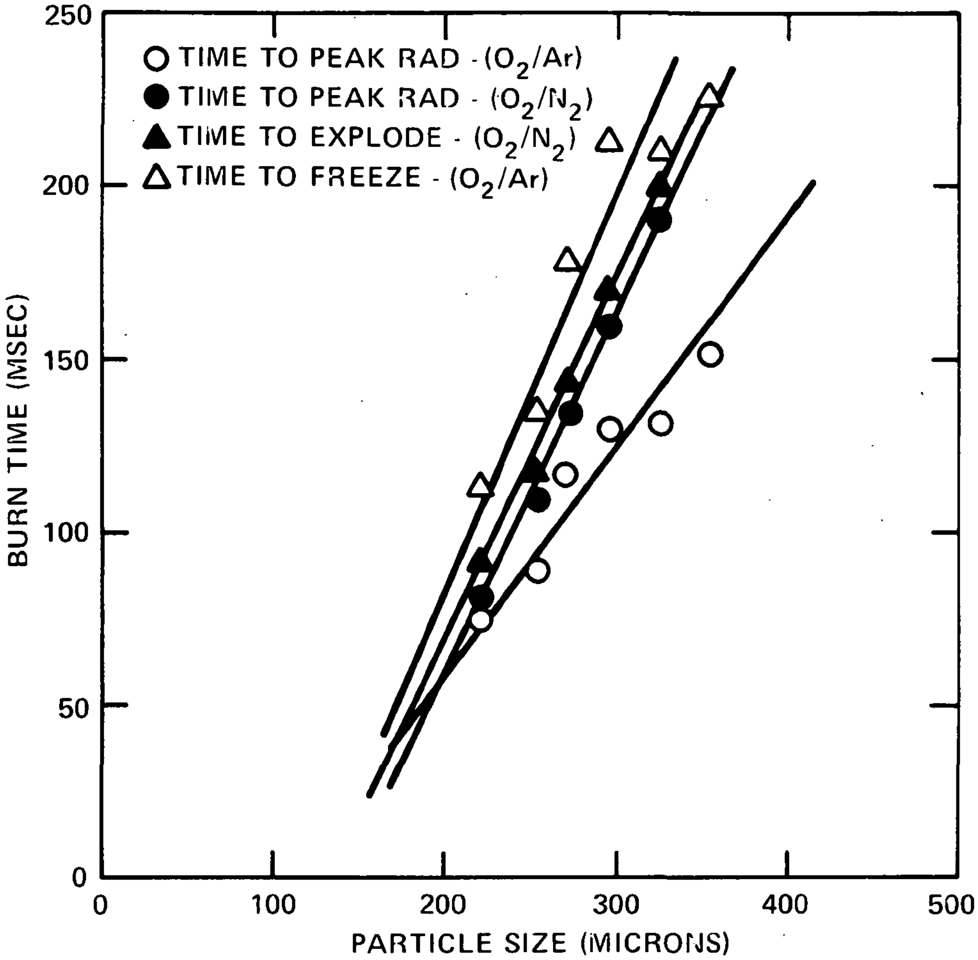

FIG. 17. Burn Time Versus Original Droplet Diameter for Be Droplets Burning in 50/50 Mixtures of O_2/Ar and O_2/N2 at 700 ±7 Torr. Data show that particles burning in O_2/N2 explode at times intermediate between "normal" t_{peak} and t_{freeze} for O_2/Ar.

The ratio of the time to freeze versus the time to peak radiation changes as a function of both O_2 concentration and droplet size and it is instructive to compare these changes for both O_2/Ar and O_2/N_2. Figure 18 shows, on one plot, the variation in the ratio $t_{freeze}/t_{peak\ rad.}$ as a function of O_2 mole fraction for 272 μm droplets as well as the variation of the ratio as a function of droplet size for a fixed O_2 concentration of 75%. Data for both O_2/Ar and O_2/N_2 are given and it may be seen that for any fixed diameter and fixed O_2 concentration the droplet freezes sooner in N_2 than in Ar. This fact, considered together with the finding that radiant emission intensities are always less in N_2 than in Ar, indicates that the droplets burn cooler in O_2/N_2. Further,

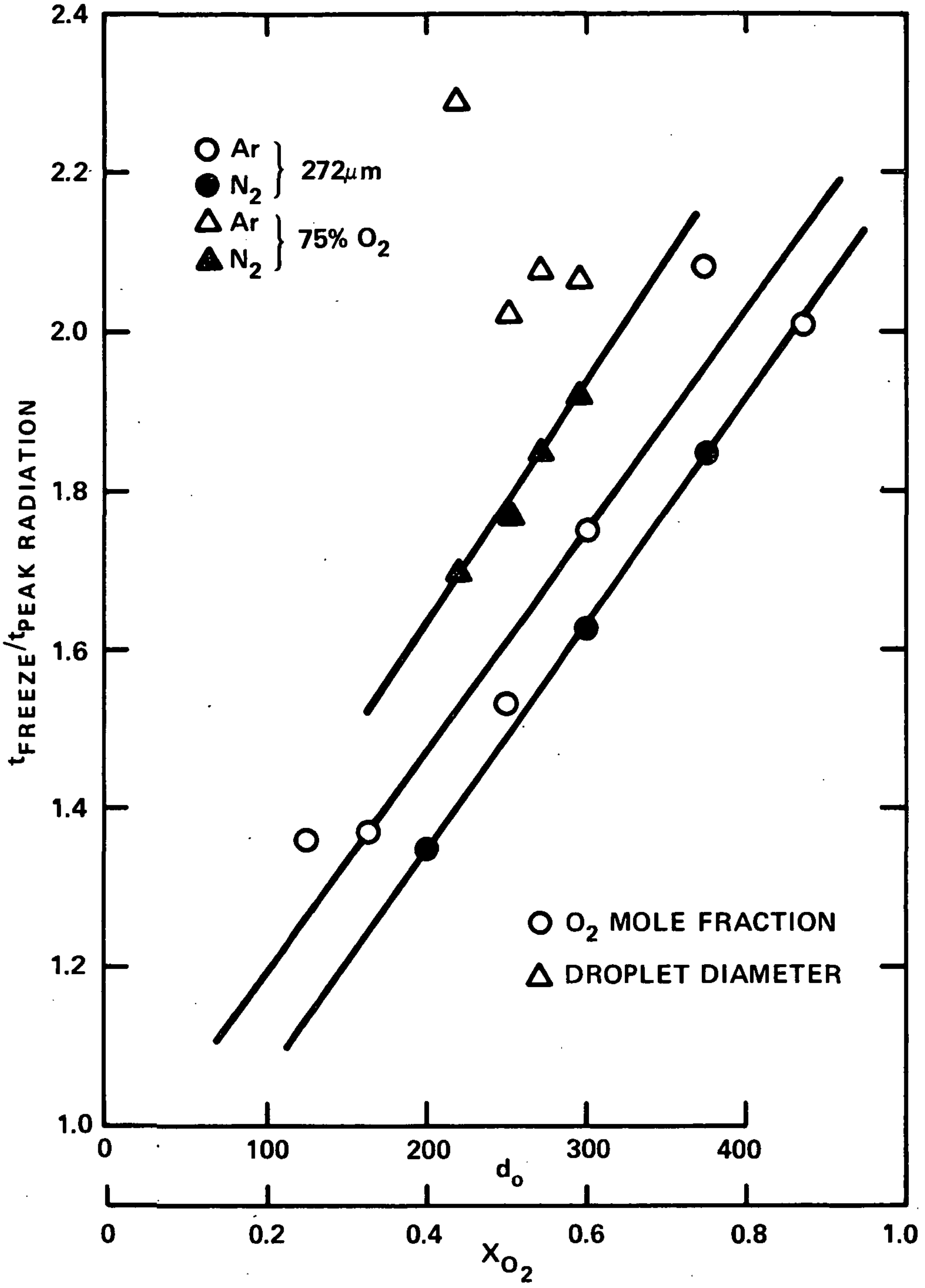

FIG. 18. Be Droplets Burned in O_2/N_2 at 700 ±7 Torr. Showing on one plot, the variation in the ratio of $t_{freeze}/t_{peak\ rad.}$ as a function of both O_2 mole fraction and droplet diameter. The plot shows clearly that the burning temperature in N_2 is lower than in Ar and thus freezing is earlier in N_2 than Ar.

the relationship appears to be linear for all except the change of $t_{freeze}/t_{pk\ rad}$ versus d_o in O_2/Ar. It has become apparent by now that, without exception, the data scatter in O_2/N_2 is always less than in O_2/Ar.

Figure 19 shows the variation in the time-to-fragmentation as a function of the original particle size. It can readily be seen that the time to explode is a linear function of the droplet diameter. Figure 20 shows the time-to-fragmentation plotted against O_2 mole fraction. There is no systematic relationship evident in these data.

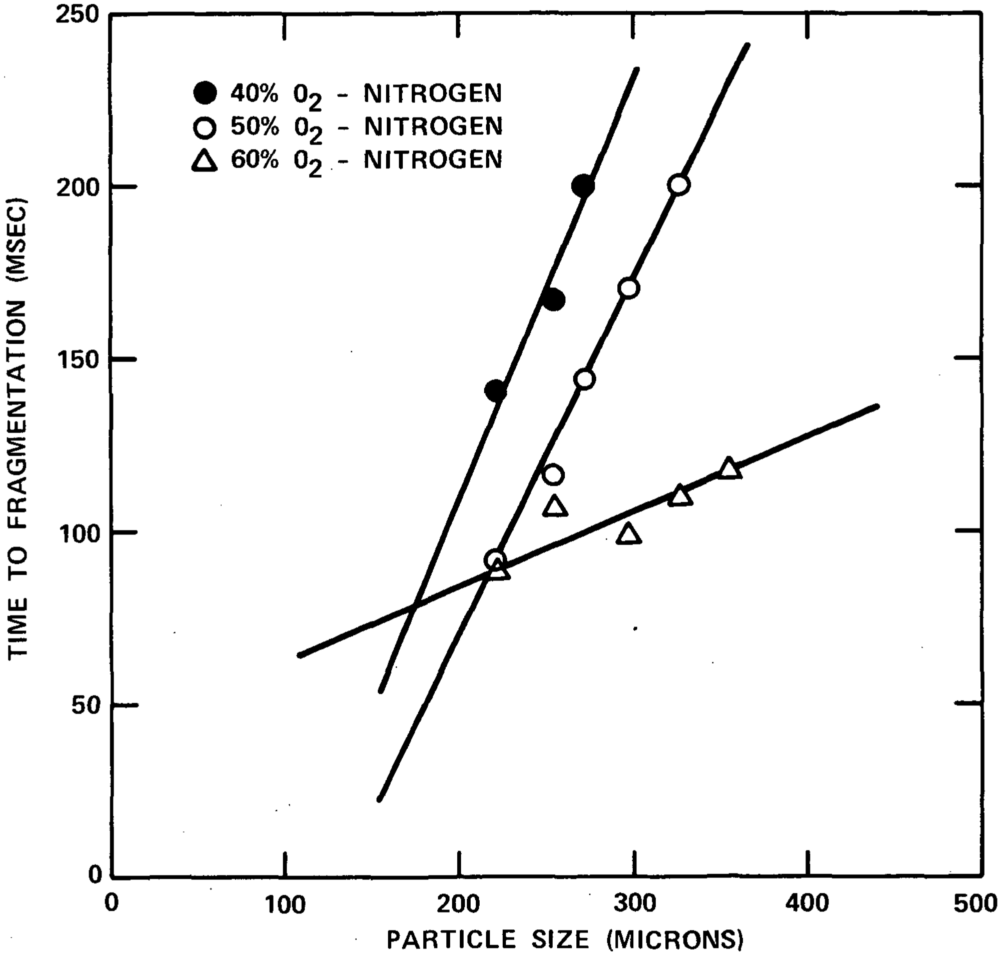

FIG. 19. Time to Fragmentation Versus Original Particle Size for Be Droplets Burned in Various O_2/N_2 Mixtures at 700 ±7 Torr.

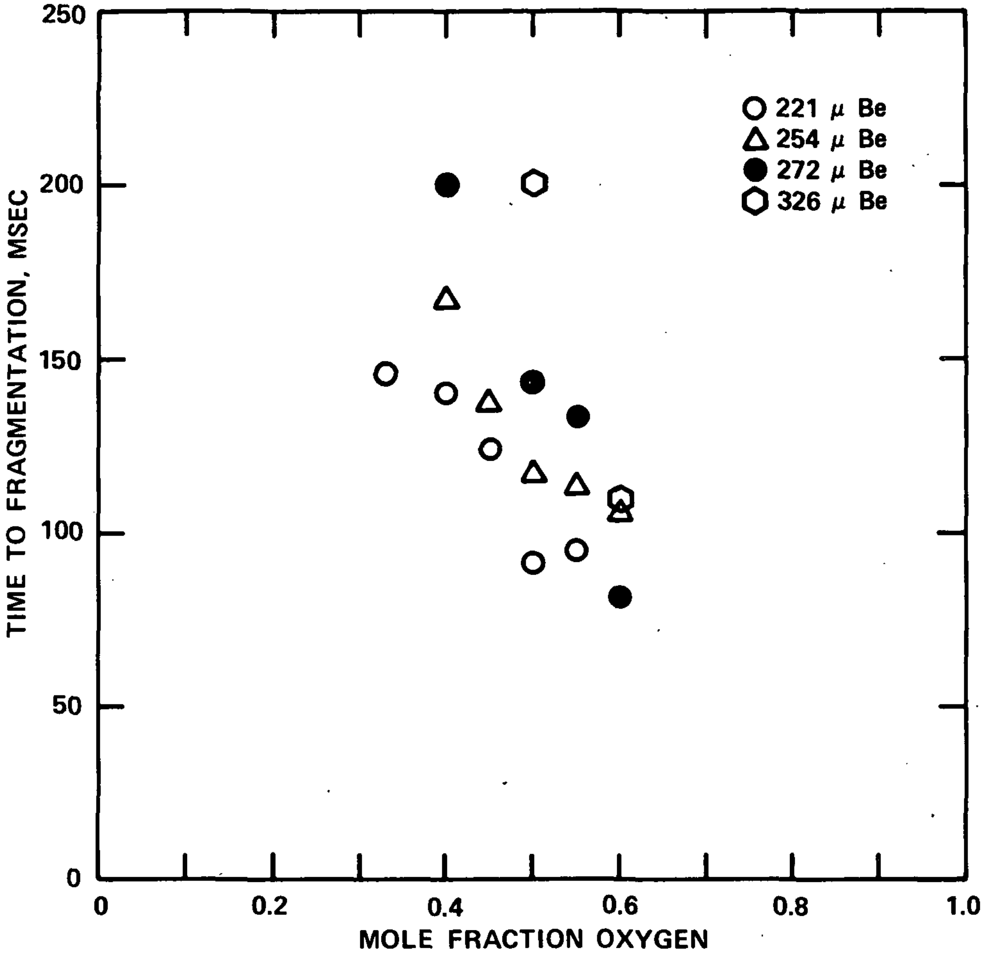

FIG. 20. Time to Fragmentation Versus O_2 Mole Fraction for Four Sizes of Be Droplets Burned in O_2/N_2 Mixtures at 700 ±7 Torr. No apparent systematic relationship exists.

As the temperature of the burning droplet rises with increasing O_2 mole fraction in O_2/N_2 mixtures the effect of reaction temperature on the nature and force of the fragmentation is readily seen. Figure 21 compares the track photos of specimens burned in O_2/N_2, showing: (a) 40% O_2/N_2, fragmentation of minimal force, few fragments, each exhibiting spearpoint; (b) 50% O_2/N_2, explosion of greater force and symmetry, *virtually all debris yielding spearpoint tracks; and (c) 60%* O_2/N_2, explosion of tremendous force, all material molten at explosion and debris consumed without spearpoint tracks. Though the force of the explosion and droplet temperature vary markedly with O_2 mole fraction it is also evident that all explosions of burning Be droplets occur when the droplet is liquid. More specifically, both the encapsulating oxide and the underlying metal are liquid.

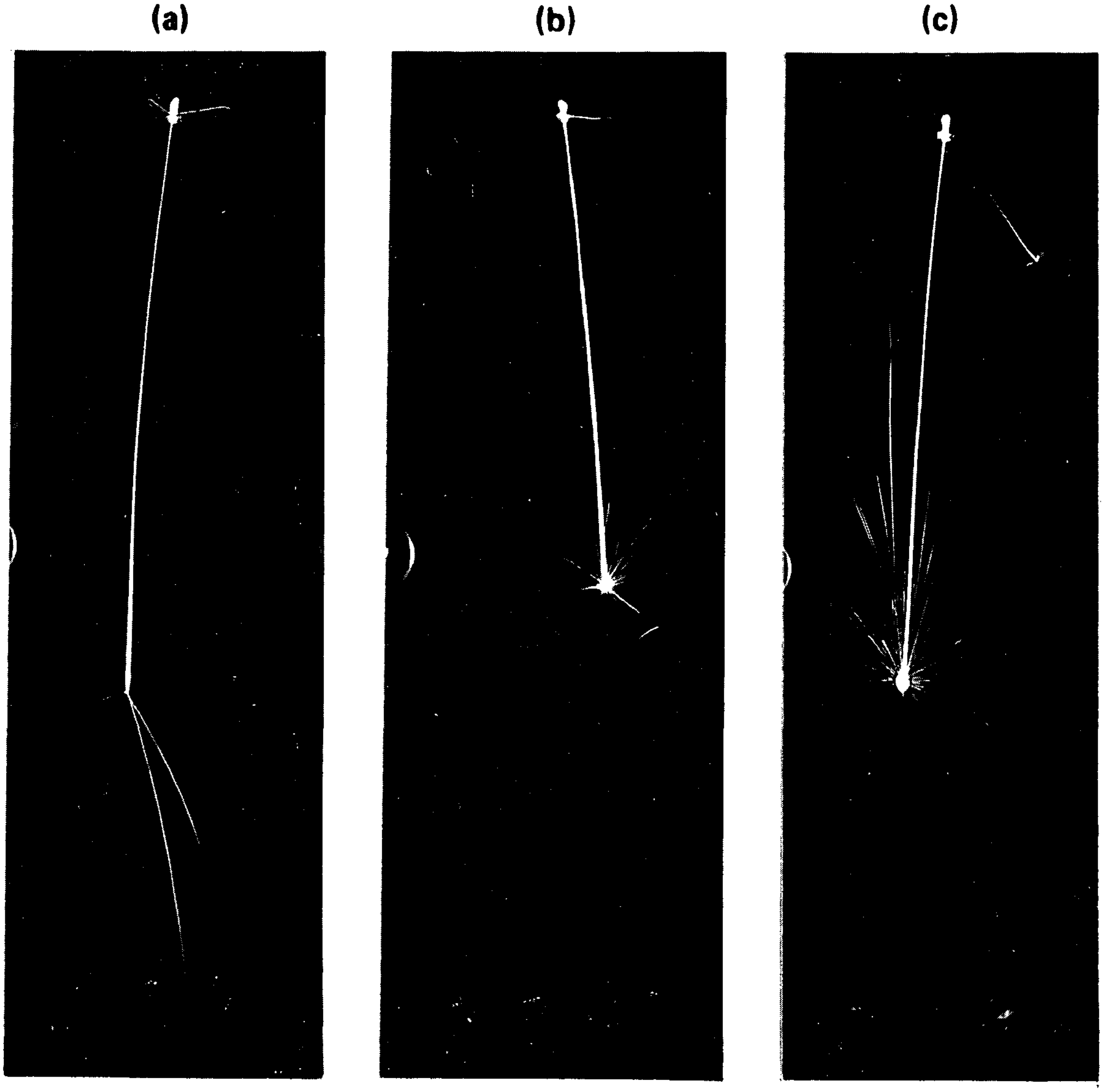

FIG. 21. Fragmentation of Be Droplets Burning in (a) 40%, (b) 50%, and (c) 60% O_2 in N_2. Note spearpoint tracks from explosion debris indicating oxide was molten at time of explosion. Quasi-steady-state droplet burning temperature increases from left to right with increasing O_2 mole fraction. Intensity of explosion and viscosity of products correlates with X_{O_2}.

In all cases of Be droplet combustion in dry gases where fragmentation does not occur, a single large BeO sphere remains as the dominant combustion product. Figure 22 compares the data for variation of the final diameter of the BeO sphere as a function of O_2 mole fraction. The plot shows that the sphere diameter increases linearly with O_2 mole fraction in O_2/Ar, but BeO sphere diameter is insensitive to O_2 mole fraction in O_2/N_2. The oxide sphere diameter is not only invariant with O_2 concentration but appears to equal nominal starting diameter of the Be droplet. The mechanistic implications of this phenomenon will be dealt with later during the discussion.

Previous experience has shown (Ref. 17 and 27) that when metals which explode in O_2/N_2 mixtures are prenitrided and then burned in the absence of N_2 (e.g., either pure O_2 or O_2/Ar) the droplets will also explode. Similar experiments were performed with Be in the following manner. Beryllium discs were heated in a tube furnace in dry, flowing N_2 at 800°C for a period of eight hours and then burned in various O_2/Ar mixtures (normally nonexploding system). It was immediately discovered that the nitrided metal required about 2.5 times less energy for ignition than the untreated metal. Ignition was found to be erratic and nonrepeatable at O_2 mole fractions ≤ 0.33 (untreated Be ignites in O_2/Ar at $X_{O_2} = 0.25$) and no particles were found to explode at this stoichiometry. Smooth ignition occurs at $\geq 40\%$ O_2 in Ar and all particles burn in a fashion qualitatively indistinguishable from untreated metal in O_2/Ar. All nitrided droplets were found to fragment at O_2 mole fractions of 0.75 or greater.

The time to peak radiation and time to onset of freezing (spearpoint) for prenitrided particles are slightly longer in O_2/Ar than for untreated metal burning in O_2/Ar, while the time to extinction is somewhat shorter for nitrided versus untreated metal. These trends of the prenitrided material burning in O_2/Ar correlate with behavior of untreated material in O_2/N_2 although they differ so little from O_2/Ar results as to be very nearly within the data scatter.

3.4. X-RAY CHARACTERIZATION OF INTERMEDIATES

Having established a reactive role for N_2 in the burning of Be droplets, efforts to identify the reaction intermediates were undertaken. In addition to the work just cited, where Be foils were prenitrided, several samples of reagent grade BeO and Be_3N_2 powders were mixed in simple molar ratios (BeO/Be_3N_2 = 3:1, 1:1, 1:3), pressed into 6.35 mm diameter pellets at 2.8×10^3 kg/cm^2 and fused in air with a 200 watt CO_2 laser in a graphite crucible. Pressing was necessary since the powders tended to scatter and be blown about by the intense radiation. Unfortunately, the desired bulk fusion was not accomplished but a molten surface layer was formed. Material from the fused spot on the several samples was then ground and submitted to X-ray powder diffraction analysis along with the debris from particle explosions in O_2/N_2. Reagent grade BeO and Be_3N_2 powders were X-rayed to provide standard reference patterns.

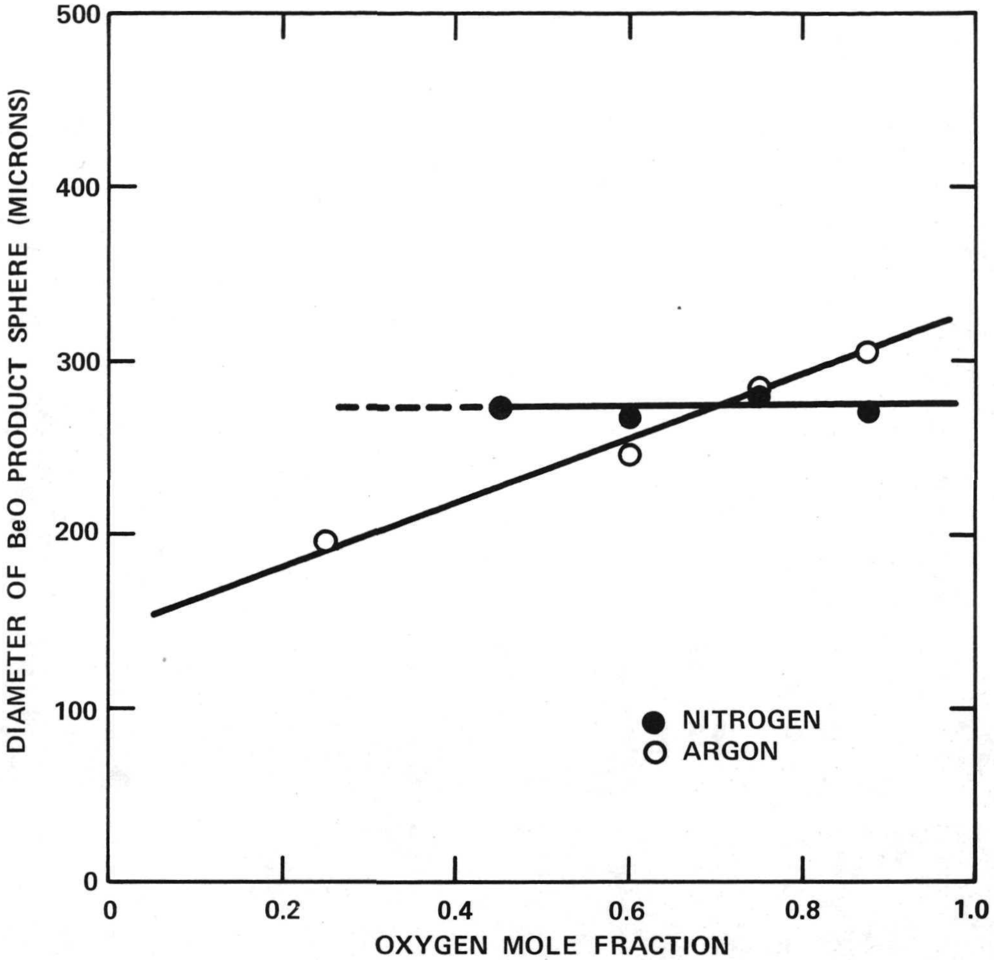

FIG. 22. Burnt Sphere Diameter (BeO) Versus O_2 Mole Fraction for Be Droplets Burned in Mixtures of O_2/Ar and O_2/N_2 at 700 ±7 Torr. Each data point is mean of five replicate experiments. Note that BeO sphere generated in N_2 equals nominal Be starting diameter and its size is insensitive to O_2 mole fraction.

Reproductions of the powder patterns of the various products are shown in Fig. 23. The results of these experiments are summarized in Table 3. These experiments lead to the conclusion that one or more new species, not BeO or Be_3N_2, are formed as intermediates during reactions leading to explosion of Be droplets in O_2/N_2 mixtures. Fusion of Be_3N_2 in air yields an oxynitride provisionally identified as $BeO \cdot 3Be_3N_2$.

Our efforts to synthesize the intermediates have not yielded identical powder patterns to the debris from particle explosions. A possible explanation of these results would include the following. Since so little debris is collected from each particle explosion the material from numerous specimens burned over the whole range of explosion

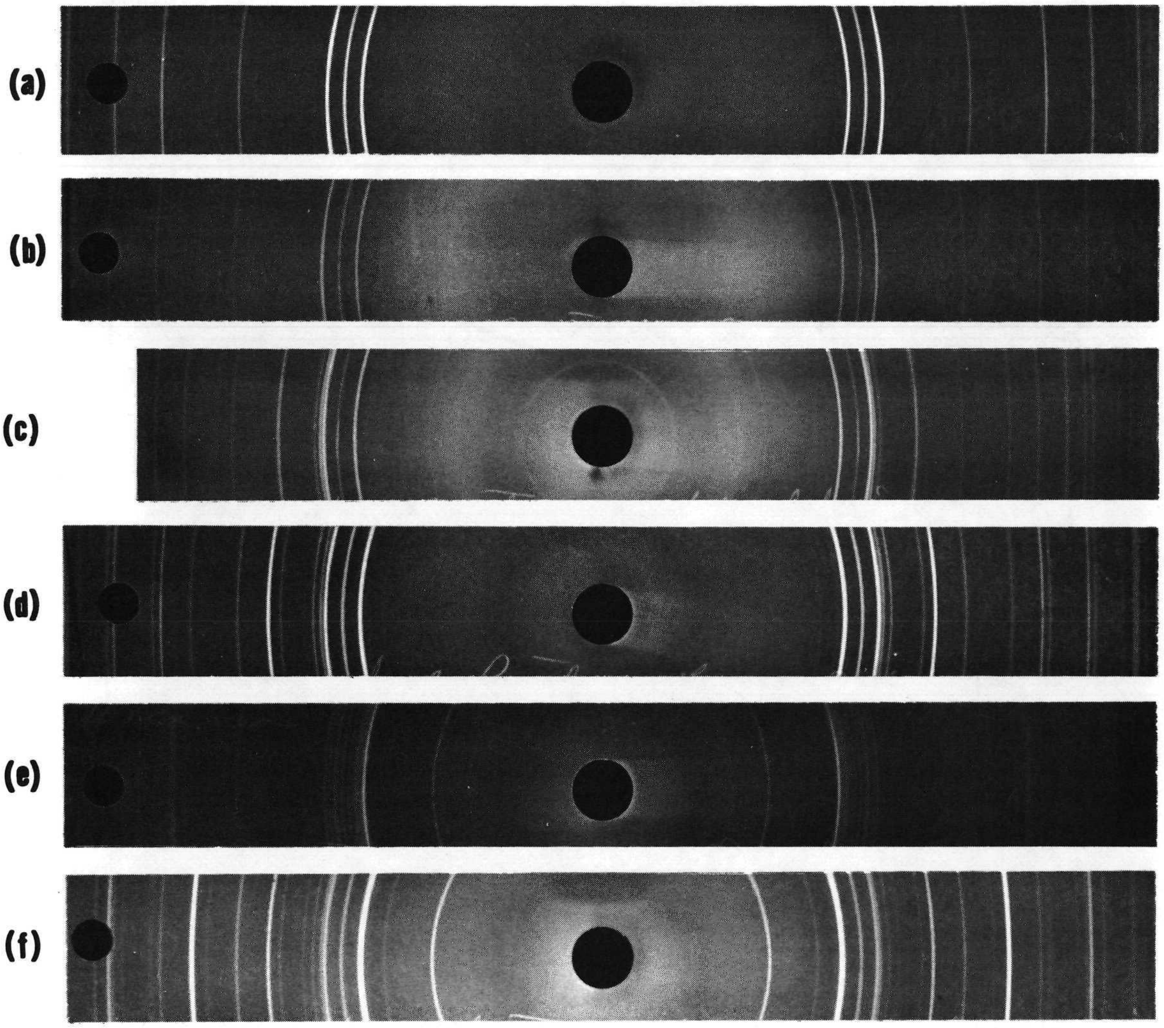

FIG. 23. X-ray Powder Diffraction Patterns of Species in the Combustion of Be Droplets in O_2/N_2 Mixtures. (a) Reagent grade BeO, reference pattern, (b) oxide spheres from Be burning in O_2/Ar, (c) debris from explosions in O_2/N_2, (d) unexploded spheres from Be burning in O_2/N_2 mixtures outside explosion limits, (e) fused reagent powder compact of $BeO:3Be_3N_2$, (f) reagent grade Be_3N_2, reference pattern.

stoichiometry (40-60% O_2/N_2) was collected and used for X-ray analysis. It is possible that, as a result, two or more oxynitrides are formed, as is true for Zr and Al (Ref. 28), and the powder pattern we have represents a composite specimen. The pattern does, however, indicate the presence of the $BeO \cdot 3Be_3N_2$ as one component. Termination of the contract precluded pursuit of this problem, but quite obviously, further work needs to be done in this area. Adequate samples for X-ray analysis should be prepared at 40, 50 and 60% O_2 in N_2. X-ray study of the material resulting from N_2 plasma-fusion of premixed oxide-nitride powder compacts would also be illuminating.

TABLE 3. Summary of X-Ray Powder Diffraction Analysis of Intermediate Reaction Products in the System $Be/O_2/N_2$.

Starting material	Treatment (experiment)	Product expected	Product found (X-ray)
BeO (reagent)	None	...	BeO
Be_3N_2 (reagent)	None	...	Be_3N_2 (trace BeO)
Explosion debris	Burned in O_2/N_2	BeO_xN_y	BeO_xN_y (2 or more incl. $BeO \cdot 3Be_3N_2$)
Unexploded spheres	Burned in O_2/Ar	BeO	BeO
Prenitrided Be	N_2 soak at 800°C	α-Be_3N_2	α-Be_3N_2
Pressed pellet ($3BeO/Be_3N_2$)	Laser fusion in air	BeO_xN_y	$BeO \cdot 3Be_3N_2$
Pressed pellet (BeO/Be_3N_2)	Laser fusion in air	BeO_xN_y	$BeO \cdot 3Be_3N_2$
Pressed pellet ($BeO/3Be_3N_2$)	Laser fusion in air	BeO_xN_y	$BeO \cdot 3Be_3N_2$
Be_3N_2 (reagent)	Laser fusion in air	β-Be_3N_2	$BeO \cdot 3Be_3N_2$

3.5. SUMMARY OF BURNING IN OXYGEN/NITROGEN

The evidence for the reaction of N_2 with burning Be droplets is unequivocal. Nitrogen is shown to affect the ignition limit and to retard the combustion. The presence of N_2 has been shown to induce droplet fragmentation while in its absence no explosions occur.

The retardation process has three basic manifestations: (1) the ignition limit (i.e., X_{O_2} necessary for ignition at fixed energy input) is higher in N_2 relative to Ar, (2) the burning rate is lowered, and (3) final BeO sphere diameter is unaffected by changes in O_2 mole fraction in O_2/N_2. Here we encounter a situation where, even though O_2 and N_2 are both reactants, one retards reaction of the other.

We have shown previously (Ref. 17) that both vapor phase and surface combustion processes occur simultaneously during the burning of Be droplets. Dramatic and chaotic growth of oxide can in fact occur prior to melting of the metal foil into a droplet (Ref. 11). Thus the heat release necessary to achieve ignition and vigorous combustion must come from both of these processes.

Beryllium nitride and BeO are both thermodynamically probable reaction products. We have shown (Section 3-4) the formation of a nitride on heated foils at 800°C. Gulbransen and Andrew (Ref. 26) have shown that the presence of a nitride film on Be has a negligible effect on the Be vapor pressure relative to an oxide film. For example, an oxide skin 0.04 μm thick reduced the Be vapor pressure by a factor of 60, while a nitride skin of 0.16 μm reduced the Be vapor pressure by only a factor of 4 (i.e., skin thickness of BeO/Be_3N_2 in the ratio 1:4 reduces Be vapor pressure in the ratio 15:1). If the vapor phase reaction is not significantly altered yet the ignition and later combustion are retarded then the surface process must be inhibited.

If we assume that the initial oxidation mechanism is like at least two other elements of Group IIA (magnesium and barium, Ref. 29), then under normal conditions, the sticking probability of O_2 increases as oxidation progresses. Under the conditions of these droplet burning studies a nitride film or crust, permeable to Be vapor, must form which alters the sticking coefficient of O_2 and thus degrades the reaction processes generating heat at the droplet surface. The practical consequences, manifest in the experimental results, are as follows: (1) at fixed particle size, higher O_2 concentration is necessary to raise the surface temperature to ignition in N_2 relative to Ar, and (2) at constant O_2 concentration, droplet temperature and thus burning rate is lower (burn time longer) in N_2 relative to Ar. The overall effect on the burning temperature can be seen in the photomultiplier records and still plate track photos which show greatly reduced radiant emission intensity from the particles as well as sharper, less diffuse tracks in N_2 relative to Ar. Additionally, Fig. 18 shows that the ratio of $t_{\text{freeze}}/t_{\text{peak rad.}}$ is lower in N_2 relative to Ar, both as a function of O_2 concentration and droplet diameter.

One further experimental fact showing a surface effect for N_2 is the difference in behavior of the sphere forming process shown in Fig. 22. Outside the explosion limits encapsulation is the net effect whether burning in O_2/Ar or O_2/N_2. In O_2/Ar the sphere size increases with increasing O_2 concentration. The BeO sphere may be less than or greater than d_o. In O_2/N_2 sphere size is insensitive to O_2 mole fraction and remains constant within ±5% of d_o. The Pilling-Bedworth ratio (i.e., molecular volume of oxide/volume of gfw metal) of both the nitride and the oxide of Be are significantly greater than 1.0 and thus substantial metal would be lost from the droplet even in the case of the final sphere diameter equaling d_o. It seems apparent that, after some metal loss due to vaporization, the nitride stabilizes the surface geometry in some way which causes reaction to propagate from an established surface inward, but the microscopic details of the process remain unclear.

The fragmentation of Be droplets is seen to have the attributes of all the other metals (Al, Ti, and Zr) whose burning droplets are known to explode: explosions occur in O_2/N_2 mixtures but not in O_2/Ar, oxide balloons are blown at the explosion threshold, time to explode is a linear function of original droplet diameter and the droplets, practically without exception, are molten at the time of fragmentation. Beryllium, unlike the others, has both upper and lower thresholds of N_2 concentration for droplet explosion.

The last word is not in yet on the mechanism of fragmentation of burning metal droplets but a consistent body of experimental evidence is accumulating and a cogent theoretical argument on the nucleation process has recently been published (Ref. 30). Extensive studies at the Sandia Laboratories (Ref. 22, 27, 28, 31, and 32) on the combustion and fragmentation of Zr droplets in the presence of N_2 have identified N_2 gas in the oxide balloons or sacs blown under threshold conditions and have implicated Zr oxynitrides as active intermediates. In the work of Meyer and Brieland (Ref. 33) when Zr prenitrided with $^{30}N_2$ was burned in mixtures of $O_2/^{28}N_2$, the resultant gas found in the sacs blown at the explosion threshold was $^{29}N_2$. Three distinct oxynitrides of both Al and Zr have been synthesized by Gilles (Ref. 28) and characterized by X-ray spectroscopy. This study reveals the presence of two or more oxynitrides of Be. Stable nitrides (a necessary precursor) of all of these metals are predicted on thermodynamic grounds.

The evidence is overwhelming that these metal droplet fragmentations are gas driven. While N_2 is not the only gas capable of initiating such explosions (there is a CO/oxycarbide analog, Ref. 17) the studies cited here, using N_2, show that the driving force for the explosion comes mainly from oxynitride-derived N_2 with an assist from metal vapor and any volatile suboxides which may be present.

The main criticism of such a mechanism has been that, according to simple homogeneous nucleation theory, overpressures in the neighborhood of 50 atmospheres were necessary for droplet rupture. Best estimates of the pressures available from the mechanism suggested here run around 1.5 atmospheres. Clearly, a serious discrepancy exists. Levine (Ref. 30) recently applied the theory of homogeneous bubble nucleation to the Zr bubble forming process. Based on estimated properties of the Zr-O-N melt, an unusually high vapor pressure was found necessary to form a critical vapor nucleus. Levine then postulated the existence of a chemisorbed layer at the surface of the vapor embryos and showed that a much lower vapor pressure would be required if the effects of chemisorption were incorporated into the nucleation theory. As a result of this analysis calculated overpressures are brought into order-of-magnitude agreement with experiment. This is a nucleation model and, as it stands, it says nothing about particle diameter. In every known case of droplet explosion the time to explode is a linear function of droplet diameter.

The explosion mechanism offered by Meyer and Breiland is a self-accelerating thermal decomposition of metastable oxynitride plus recombination of unstable N_2 species. Nitrogen recombination is said to provide the heat to propagate the developing explosion. This mechanism has been criticized on the grounds that it requires the existence of liquid oxynitride molecules in the melt and such species have not been confirmed outside the low temperature solid state. Hopefully, an accurate synthesis is not far off which will expand on the nucleation mechanism of Levine and the propagation mechanism of Meyer and Breiland.

4. FINAL SUMMARY AND CONCLUSIONS

This study, coupled with our earlier extensive scanning electron microscopy (Ref. 14) of quenched Be particles reveals in minute detail the rates, mechanisms and evolution of morphology of single Be droplets burning in a variety of oxidizing gases. A similarity of melting and boiling points between Al and Be has, upon occasion, led the uncritical to ascribe identical burning mechanisms to both metals. The burning of droplets of these two metals is, however, only superficially similar. It has generally been acknowledged though, that, all else being equal, Be is the more difficult to ignite and has a longer burning time. The fact that BeO on the surface of the burning droplet *melts* at a temperature higher than the metal *boils* (i.e., M.P. BeO = 2820°K, B.P. Be = 2756°K) has serious consequences for efficient droplet combustion.

Aside from a difference in burning rates (Al about twice as fast as Be), Be droplet combustion differs from Al in the following basic ways:

Be droplet completely encapsulated during burning while Al has asymmetrical globule of surface oxide.

Small quantities of water vapor in the environment ($\sim$2%) change physical properties of surface Al_2O_3 only slightly; Be droplets burn with a clean surface in water vapor and no large solid oxide spheres result.

This study and Ref. 13, 17, and 18 from our laboratory have shown that Be droplet combustion is extremely sensitive to the chemistry of environmental species. Nitrogen has been shown to have a dramatic effect on the burning of these Be droplets by raising the ignition limit and reducing the burning rate (lengthening burn time) in mixtures of O_2/N_2 relative to O_2/Ar. This study presents the first documentation of the phenomenon of droplet fragmentation for Be. Nitrogen-induced fragmentation terminates combustion in slightly less than half the "normal" burn time in O_2/Ar. Particles burning in O_2/N_2 outside the explosion limits have burn-out times 16% longer than those in O_2/Ar. Nitrogen affects the terminal droplet size and fixes it at nominal d_o, apparently by affecting the mechanism as well as the morphology of the concurrent surface reaction. The sum of these results and our previous systematic studies of Be burning in O_2/Ar demonstrate conclusively and unequivocally that: (a) N_2 is not inert in metal combustion processes, and (b) as a consequence of the obvious condensed phase processes occurring during Be droplet combustion, a burning model which makes no attempt to describe oxide buildup on the droplet and employs only simple gas-phase kinetics, is hopelessly inadequate.

Appendix A

SUMMARY OF EXPERIMENTS FOR WHICH DATA WERE TAKEN

Beryllium Burning in O_2/Ar (Dry)

Original Droplet Diameter	Mole Fraction Oxygen								
	.20	.25	.33	.40	.50	.60	.75	.875	1.00
221μm			x		x		x		
254μm			x		x		x		
272μm		x	x		x	x	x	x	x
296μm					x		x		
326μm		x		x	x	x			
354μm			x	x	x	x	x		

Beryllium Burning in O_2/N_2 (Dry)

Original Droplet Diameter	Mole Fraction Oxygen								
	.25	.33	.40	.45	.50	.55	.60	.75	.875
221μm	x	x	x	x	x	x	x	x	x
254μm	DNI	x	x	x	x	x	x	x	x
272μm	DNI	DNI	x	x	x	x	x	x	x
296μm	DNI	DNI	x	x	x	x	x	x	x
326μm	DNI	DNI	x		x	x	x		Burst
354μm	DNI	DNI	DNI				x		Burst

x = data taken
DNI = does not ignite
Burst = ruptures under irradiation

Appendix B

BERYLLIUM PARTICLE COMBUSTION IN OXYGEN/ARGON

Burn time vs. mole fraction oxygen for 221 μ beryllium particles burning in oxygen-argon mixtures (700 ±7 torr) (all times in milliseconds).

X_{O_2}	t_{peak}	t_{freeze}	$t_{extinct}$	BeO sphere diameter, μ
.333	131	189	324	214
.333	119	169	328	207
.333	128	180	333	209
.500	75	106	208	203
.500	72	110	223	213
.500	72	116	250	247
.500	78	115	245	253
.500	77	118	252	253
.750	43	91	190	...
.750	37	90	186	246
.750	38	103	200	212
.750	42	91	182	208
.750	50	102	189	234

Burn time vs. mole fraction oxygen for 254 μ beryllium particles burning in oxygen-argon mixtures (700 ±7 torr) (all times in milliseconds).

X_{O_2}	t_{peak}	t_{freeze}	$t_{extinct}$	BeO sphere diameter, μ
.333	150	216	379	236
.333	144	206	384	233
.333	153	222	367	242
.333	150	...	...	...
.500	89	135	300	255
.500	92	129	275	241
.500	83	140	273	239
.500	88	135	285	...
.750	55	115	210	167
.750	58	116	228	249
.750	54	108	235	250
.750	60	118	233	...

BERYLLIUM PARTICLE COMBUSTION IN O_2/AR

Burn time vs. mole fraction oxygen for 272 μ beryllium particles burning in oxygen-argon mixtures (700±7 torr) (all times in milliseconds).

X_{O_2}	t_{peak}	t_{freeze}	$t_{extinct}$	BeO sphere diameter, μ
.250	257	362	∿530	196
.250	259	358	...	...
.250	258	330	...	...
.333	186	254	410	...
.333	180	255	460	269
.333	192	243	420	...
.333	188	264	450	...
.333	175	...	...	...
.333	183	257	403	...
.500	110	162	330	...
.500	125	200	350	...
.500	118	175	...	...
.500	113	177	...	...
.600	80	140	250	251
.600	85	144	262	241
.600	77	140	245	...
.750	70	142	220	279
.750	68	136	225	281
.750	71	135	255	...
.750	66	151	269	302
.750	68	147	267	280
.875	59	148	205	285
.875	73	139	...	325
.875	65	105	...	...
1.000	58	121	240	...

BERYLLIUM PARTICLE COMBUSTION IN O_2/AR

Burn time vs. mole fraction oxygen for 296 μ beryllium particles burning in oxygen-argon mixtures (700 ±7 torr) (all times in milliseconds).

X_{O_2}	t_{peak}	t_{freeze}	$t_{extinct}$	BeO sphere diameter, μ
.250	180	255	...	231
.500	130	207	375	308
.500	123	218	365	260
.500	136	217	360	304
.500	121	215	370	...
.750	78	167	288	312
.750	75	153	324	327
.750	89	181	350	295
.750	...	...	...	340

Burn time vs. mole fraction oxygen for 326 μ beryllium particles burning in oxygen-argon mixtures (700±7 torr) (all times in milliseconds).

X_{O_2}	t_{peak}	t_{freeze}	$t_{extinct}$	BeO sphere diameter, μ
.250	190	267	...	231
.400	169	248	...	302
.400	139	262	...	270
.400	150	220	...	...
.400	155	250	...	...
.500	139	209	...	292
.500	122	213	...	310
.500	128	202	...	298
.500	136	215	...	...
.600	130	232	430	336
.600	128	230	460	340
.600	127	230	470	305
.600	130	243	...	...
.875	90	184	∿350	...

BERYLLIUM PARTICLE COMBUSTION IN O_2/AR

Burn time vs. mole fraction oxygen for 354 μ beryllium particles burning in oxygen-argon mixtures (700 ±7 torr) (all times in milliseconds).

X_{O_2}	t_{peak}	t_{freeze}	$t_{extinct}$	BeO sphere diameter, μ
.333	258	347	...	308
.400	195	274	...	301
.400	195	272	...	325
.400	198	283	...	...
.500	141	210	...	295
.500	158	230	...	319
.500	158	238	...	...
.600	110	208	...	313
.600	140	242	...	342
.600	125	230	...	336
.600	125	242	...	346
.750	125	231	...	375
.750	123	235	...	373
.750	120	238	...	...
.750	119	212	...	...

Appendix C

BERYLLIUM PARTICLE COMBUSTION IN OXYGEN/NITROGEN

Burn time vs. mole fraction oxygen for 221 μ beryllium particles burning in O_2/N_2 mixtures (700 ±7 torr) (all times in milliseconds).

X_{O_2}	t_{peak}	$t_{explode}$	t_{freeze}	$t_{extinct}$	BeO sphere diameter, μ
.25	65	...	...	175	...
.25	70	...	...	339	...
.33	132	136	...	...	...
.33	144	...	195	272	...
.33	142	147	...	...	...
.33	...	156	...	...	...
.40	128	135	...	...	...
.40	133	...	180	292	215
.40	130	136	...	...	...
.40	141	148	...	...	...
.45	120	126	...	...	...
.45	115	121	...	...	...
.45	119	124	...	...	...
.50	84	88	...	...	...
.50	81	85	...	...	...
.50	89	92	...	...	...
.50	94	97	...	...	...
.55	83	87	...	...	...
.55	93	99	...	...	...
.55	92	96	...	...	...
.55	94	99	...	...	...
.60	68	...	100	166	...
.60	66	...	113	...	...
.60	71	...	108	217	245
.60	83	89	...	...	...
.75	69	...	108	220	215
.75	68	...	122	213	210
.75	64	...	112	223	213
.875	41	...	79	150	balloon (shattered)
.875	49	...	95	180	N.R.
.875	42	...	84	175	242
.875	52	...	92	175	285 (balloon)

BERYLLIUM PARTICLE COMBUSTION IN O_2/N_2

Burn time vs. mole fraction oxygen for 254 μ beryllium particles burning in O_2/N_2 mixtures (700 ±7 torr) (all times in milliseconds).

X_{O_2}	t_{peak}	$t_{explode}$	t_{freeze}	$t_{extinct}$	BeO sphere diameter, μ
.33	180	...	234	363	...
.33	189	...	210	349	...
.33	DNI	...	...	...	...
.33	DNI	...	...	...	...
.40	162	171	...	...	...
.40	168	172	...	...	...
.40	150	158	...	...	...
.40	161	167	...	...	261 (balloon)
.45	132	139	...	...	...
.45	128	134	...	...	...
.45	132	137	...	...	...
.50	112	119	...	...	...
.50	109	115	...	...	...
.50	110	115	...	...	...
.55	...	86	...	...	...
.55	112	116	...	...	...
.55	100	108	...	...	...
.55	108	116	...	...	...
.60	92	97	...	...	...
.60	89	102	116	207	...
.60	100	108	141	288	...
.60	88	117	...	...	...
.75	68	...	124	260	245
.75	69	...	128	269	243
.75	71	...	107	250	234
.75	74	...	140	277	268
.875	68	...	132	275	N.R.
.875	50	...	112	250	N.R.
.875	59	...	122	271	258
.875	58	...	116	265	267

BERYLLIUM PARTICLE COMBUSTION IN O_2/N_2

Burn time vs. mole fraction oxygen for 272 μ beryllium particles burning in O_2/N_2 mixtures (700 ±7 torr) (all times in milliseconds).

X_{O_2}	t_{peak}	$t_{explode}$	t_{freeze}	$t_{extinct}$	BeO sphere diameter, μ
.33	DNI	...	...	...	...
.33	DNI	...	...	...	...
.33	DNI	...	...	...	...
.33	DNI	...	...	...	...
.40	190	196	...	...	...
.40	192	200	...	...	...
.40	200	(205)	270	450	331
.45	177	(184)	239	395	274
.45	171	178	...	...	...
.45	162	177	...	...	...
.45	155	166	...	...	...
.50	136	143	...	...	...
.50	139	148	...	...	...
.50	132	139	...	...	...
.50	131	140	...	...	...
.55	122	130	...	...	...
.55	132	138	...	...	...
.55	126	132	...	...	...
.60	...	73	...	...	...
.60	100	135	...	...	...
.60	97	...	169	310	267
.60	102	...	154	293	...
.60	...	82	...	...	...
.60	...	81	...	...	...
.75	75	...	127	255	N.R.
.75	83	...	160	300	278
.75	87	...	159	300	N.R.
.75	83	...	160	290	283
.875	68	...	132	273	279
.875	68	...	128	270	259
.875	80	...	150	290	...
.875	75	...	136	265	274

BERYLLIUM PARTICLE COMBUSTION IN O_2/N_2

Burn time vs.mole fraction oxygen for 296 μ beryllium particles burning in O_2/N_2 mixtures (700 ±7 torr) (all times in milliseconds).

X_{O_2}	t_{peak}	$t_{explode}$	t_{freeze}	$t_{extinct}$	BeO sphere diameter,μ
.33	DNI	...	...	...	...
.33	DNI	...	...	...	...
.33	DNI	...	...	...	...
.33	DNI	...	...	...	...
.40	264	...	292	...	...
.40	245	...	312	...	N.R.
.40	244	...	321	...	...
.40	228	...	300	...	311
.45	196	...	265	...	N.R.
.45	195	...	258	...	...
.45	188	...	264	...	...
.45	204	...	285	...	...
.50	170	178	...	...	...
.50	158	169	...	...	...
.50	156	168	...	...	...
.50	157	170	...	...	...
.55	173	180	...	...	...
.55	172	181	...	...	...
.55	163	172	...	...	...
.60	...	95	...	...	...
.60	...	100	...	...	...
.60	...	102	...	...	...
.60	...	97	...	...	...
.60	...	95	...	...	...
.75	95	...	183	397	318
.75	94	...	180	360	301
.875	82	...	160	319	336
.875	83	...	158	315	N.R.
.875	80	...	160	325	308
.875	76	...	161	332	296

BERYLLIUM PARTICLE COMBUSTION IN O_2/N_2

Burn time vs. mole fraction oxygen for 326 μ beryllium particles burning in O_2/N_2 mixtures (700 ±7 torr) (all times in milliseconds).

X_{O_2}	t_{peak}	$t_{explode}$	t_{freeze}	$t_{extinct}$	BeO sphere diameter, μ
.50	191	200	...	...	...
.50	182	191	...	...	...
.50	200	208	...	...	...
.55	177	190	...	...	...
.55	178	189	...	...	...
.55	178	188	...	...	...
.60	...	106	...	...	...
.60	100	107	...	...	...
.60	108	114	...	...	...

Burn time vs. mole fraction oxygen for 354 μ beryllium particles burning in O_2/N_2 mixtures (700 ±7 torr) (all times in milliseconds).

X_{O_2}	t_{peak}	$t_{explode}$	t_{freeze}	$t_{extinct}$	BeO sphere diameter, μ
.60	...	117	...	...	...
.60	...	114	...	...	...
.60	...	120	...	...	...

Appendix D

SUBIGNITION OXIDATION AND AGGLOMERATION OF BERYLLIUM PARTICLES

by

K. J. Kraeutle

The material used in subignition studies was spherical beryllium (Be) powder supplied by the Brush Beryllium Corp. This material also contained an appreciable amount of nonspherical Be. A preliminary sorting of particles was performed by passing the as-received Be over an inclined plane. This simple technique separates spherical from nonspherical material. The spheres had diameters between 105 and 125 µm. All subignition experiments were made in a hot stage microscope at atmospheric pressure (700 ±7 torr) with heating rates of 35°C/minute, and at temperatures between 870 and 880°C. After reaching the programmed temperature the samples were allowed to react isothermally for 30 minutes. The Be spheres could be observed with the optical microscope during the heating period. In addition, the heat-treated particles were examined in detail with the scanning electron microscope (SEM).

The first experiments were made in air and it was found that the addition of water vapor to the atmosphere caused a drastic change in the behavior of the Be. Because moist air contains three reactive species, namely oxygen, nitrogen, and water, it was decided to use dry and moist argon and oxygen respectively to facilitate the interpretation of the results. Oxygen and argon (water-pumped) were used as-received or after passing through a drying train. These experiments were followed by tests in which the gases were saturated with water vapor at 28°C. In the following, "as-received" (cylinder) gases and dried gases will be termed "dry gases" because no differences were observed between using cylinder gases and dried gases. The results obtained thus far are qualitative in nature, but they show that Be is very susceptible to reaction with water vapor at elevated temperatures (1150°K).

The photomicrographs in Fig. 1-4 show the Be particles as-received (Fig. 1a,b), after heating in dry oxygen (Fig. 2a,c,e), moist oxygen (Fig. 1c,d and Fig. 2b,d,f), dry argon (Fig. 3a,c,e and Fig. 4a,c,e), and moist argon (Fig. 1e,f, Fig. 3b,d,f, and Fig. 4b,d,f).

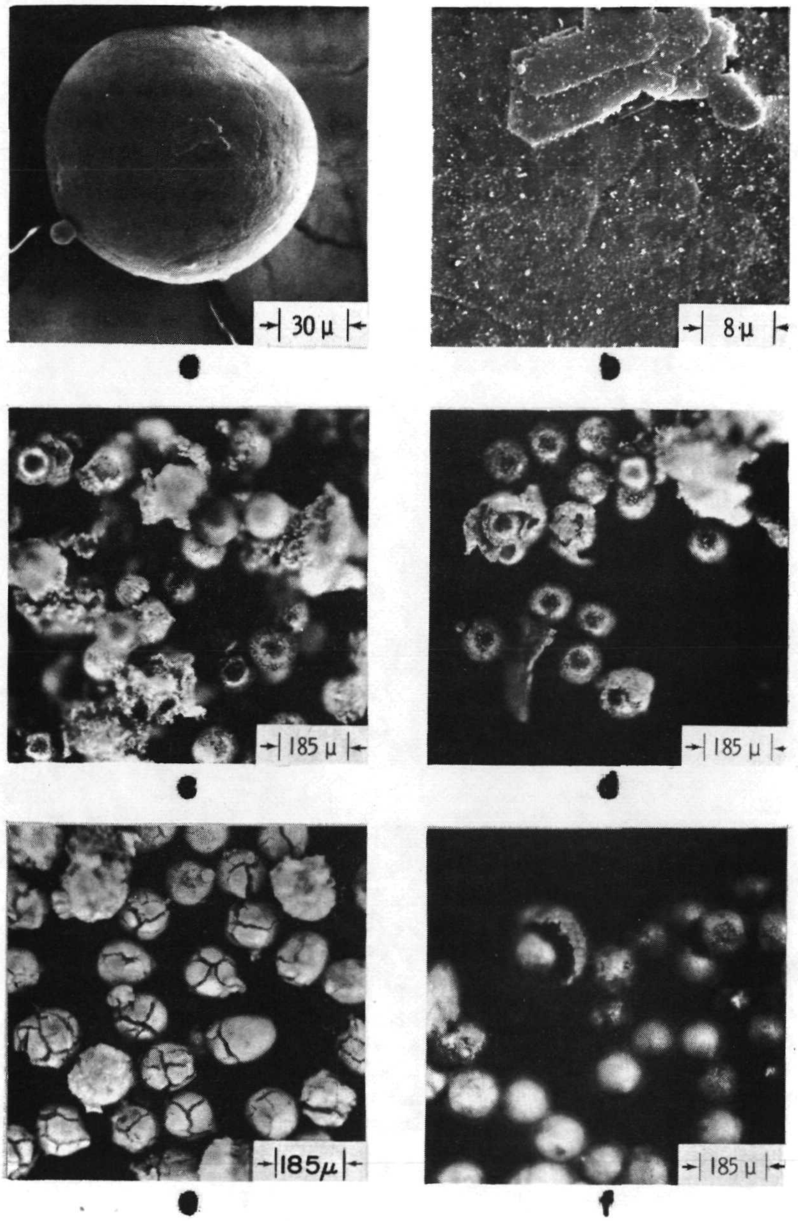

FIG. 1. Spherical Beryllium Particles (a, b) As-Received; (c, d) After Heating in Moist Oxygen; and (e, f) After Heating in Moist Argon.

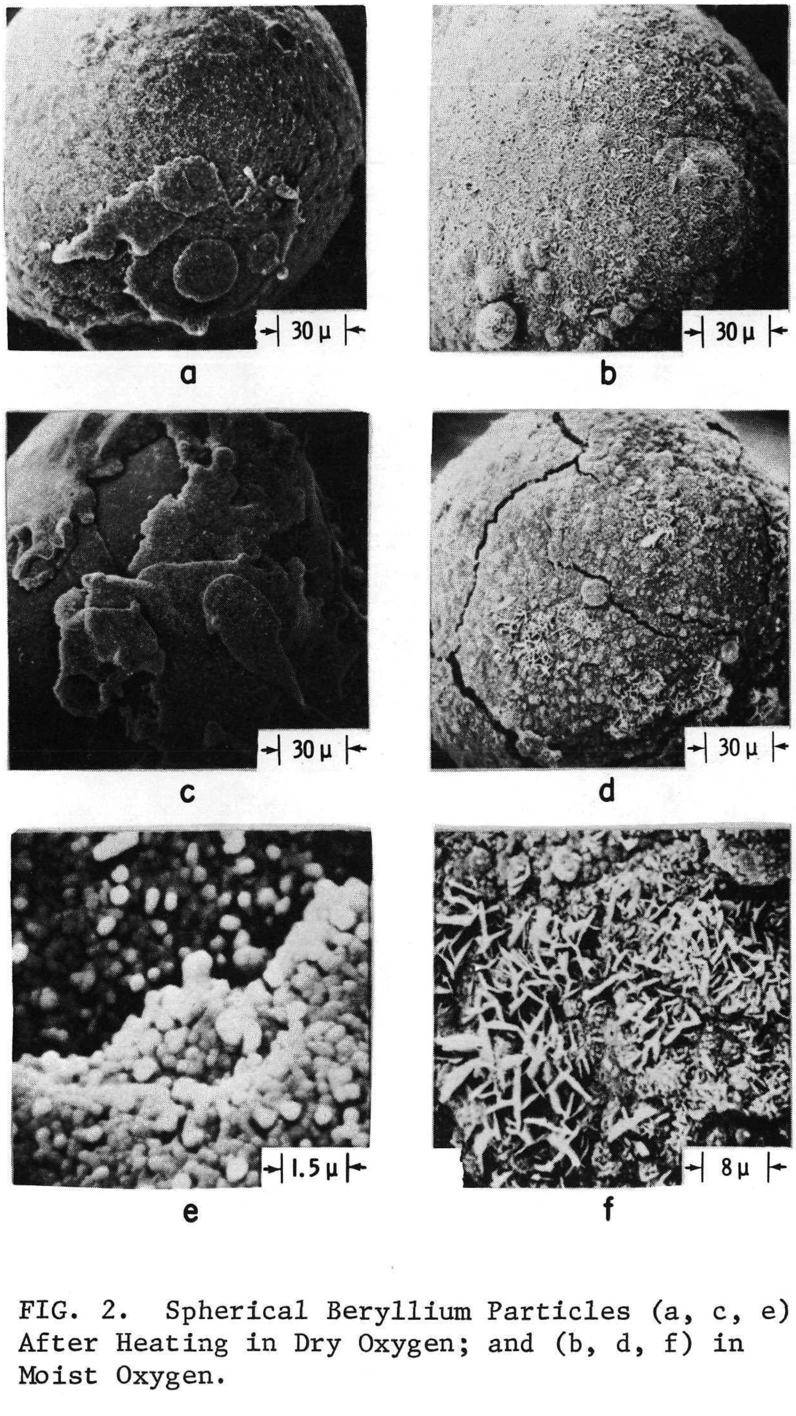

FIG. 2. Spherical Beryllium Particles (a, c, e) After Heating in Dry Oxygen; and (b, d, f) in Moist Oxygen.

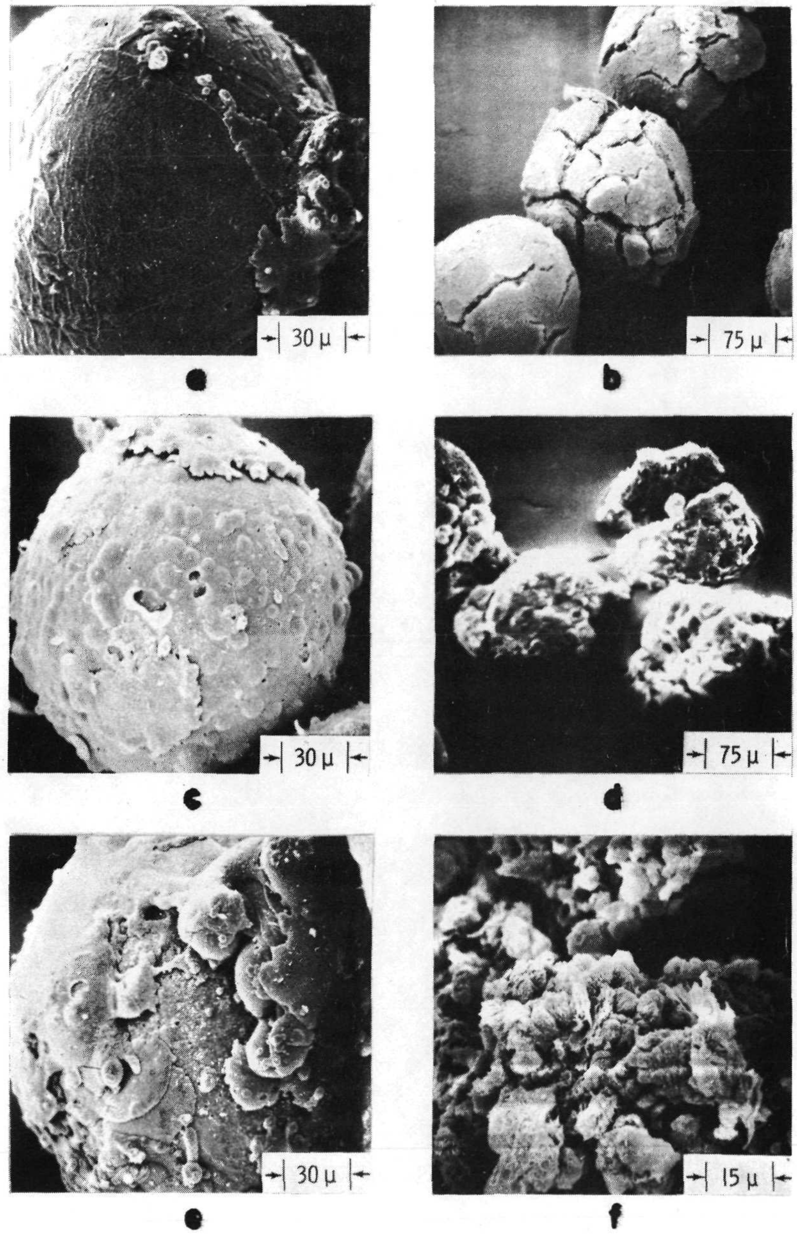

FIG. 3. Spherical Beryllium Particles (a, c, e) After Heating in Dry Argon; and (b, d, f) in Moist Argon. The four particles of photograph (d) are the fragments of a spherical particle which fell to pieces after a light touch with tweezers.

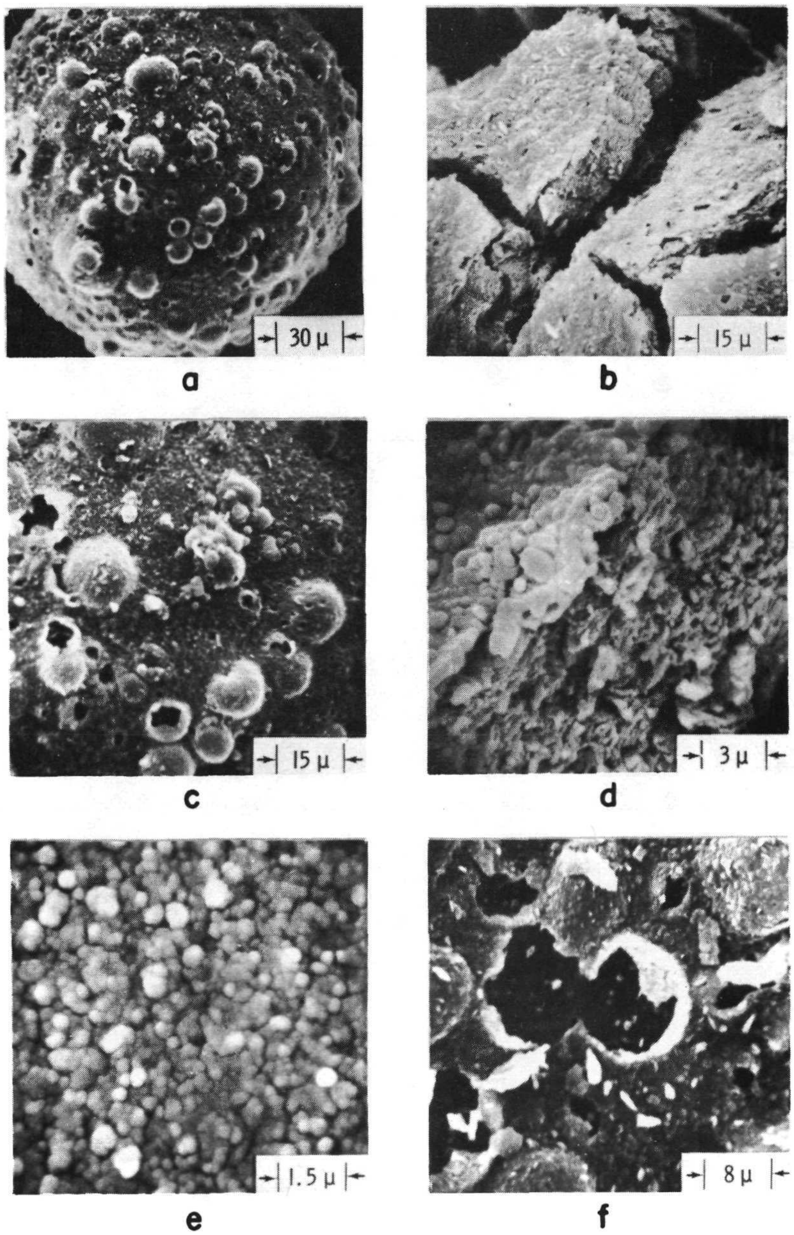

FIG. 4. Spherical Beryllium Particles (a, c, e) After Heating in Dry Argon; and (b, d, f) in Moist Argon. Picture (d) shows details of the center crack depicted in picture (b).

As-received Be particles (Fig. 1a,b) have a granular surface, buttons, and scales. One of the scales is shown in Fig. 1b. It has hexagonal structure and is presumed to be beryllium oxide (BeO) which is known to grow slowly as very thin films on compact Be during storage in air. No doubt the presence of a continuous oxide film enveloping the Be spheres accounts for the similar characteristics of particles heated in both dry oxygen and dry argon as well as the occasional peeling of the oxide film (Fig. 1d,f). The oxide can act as a barrier against further oxidation of the metal but apparently undergoes disruptive changes at the higher temperatures studied. Characteristic features of particles heated in dry argon or oxygen are the granularity of the surface (Fig. 2e and 4e) and a great number of blisters, many of which burst during heating (Fig. 3c and 4c). No blisters have been observed on as-received particles although the surface is not completely smooth (Fig. 1a,b).

A drastic change of the particle surfaces occurred as soon as the gases were saturated with water vapor. Figure 1 shows samples after heating in moist oxygen (Fig. 1c,d) and in moist argon (Fig. 1e,f). All the surfaces were very coarse. Peeling of thin layers occurred in moist oxygen as well as in moist argon. However, despite severe cracking most particles retained the original shape in moist argon. Breaking away the porous, cracked product layer usually exposed an unreacted spherical metal core. In some cases, however, the whole particle fell apart (see four slice-like segments of a particle in Fig. 3d). Figure 3f shows the fine structure of one of the segments in Fig. 3d. In moist oxygen many particles crumbled (see Fig. 1c). No pictures of the crumbled particles shown in Fig. 1c could be taken with the SEM because the sample charged too much under electron bombardment. Figures 2b, d, and f show surface details of particles which did not disintegrate in moist oxygen. Cracking was not as severe as in moist argon. Presumably the oxide is able to grow fast enough in oxygen to partially heal itself. Besides blisters and granules, the surfaces developed needles (Fig. 2d,f) which seem to be characteristic for the reaction in moist oxygen because they have not been found on particles heated in moist argon. Finally, Fig. 4 shows details of a crack (Fig. 4b, d) and some broken blisters (Fig. 4f) which developed in moist argon.

ISOTHERMAL EXPERIMENTS

The above exploratory subignition studies in dry and moist gases were continued under improved experimental conditions. Experiments were performed in a tube furnace which could be run at high temperatures for extended periods of time. The gas flow system was greatly improved with this furnace and relatively large samples of Be powder (large compared to hot stage samples) could be reacted and prepared for later use. In a typical experiment, the Be (spherical, Brush Beryllium Co., 105-125 μm diameter) was placed in a ceramic boat, the boat placed in the center of the furnace tube, and heated isothermally for different periods of time in a variety of atmospheres. The temperature was programmed at 900°C and the atmospheres were dried argon, nitrogen, oxygen (dried by passing cylinder gases through a drying train). Argon, nitrogen and oxygen were also used after being saturated at room temperature with water vapor.

Hot stage microscopy had shown earlier that the reaction of Be powder at moderate temperatures (600-800°C) is slow in dry atmospheres and that water vapor enhances the reaction dramatically. This was confirmed impressively by the large scale tube-furnace experiments. Figure 5 shows Be samples obtained after 8 hours heating at 900°C in dried argon (Fig. 5a), dried nitrogen (Fig. 5b), and dried oxygen (Fig.5c). Common to all three samples are pronounced granularity and blisters which can be broken easily by a light grinding movement. The mass of particles in each case exhibited a slight coherence which could be destroyed by slight pressure or mechanical shock. Beryllium particles heated in argon or oxygen show marked similarity (Fig. 5a, c). In nitrogen the surface seems to have developed a finer granularity (Fig. 5b). Some of the reaction product could be removed from the surface by grinding which revealed most of the metal unreacted. It is possible that much of the product layer was due to either contaminated Be or contaminated gas. This would give some explanation for the similar behavior of the samples in dry atmospheres. This point could be checked by heating the particles in vacuum.

Introduction of water vapor into the atmospheres changed the behavior of Be markedly. After 2 hours of heating at 900°C in moist argon, nitrogen, or oxygen, the Be particles had reacted almost completely. The residues of the reaction with moist argon and nitrogen were of a light grey color. The grey is attributed to tiny fragments of unreacted metal distributed throughout the reaction product. The product obtained in moist oxygen was cream-colored containing only a very small amount of unreacted material. The reaction in moist atmospheres caused the particles to crack and to break apart which led to an apparent volume increase. Figure 6 shows Be samples before (Fig. 6a) and after heating in moist argon, nitrogen, and oxygen (from top to bottom, Fig. 6b). All three samples shown in Fig. 7 were coarse and granular and similar in structure. It is evident that moist atmospheres cause severe cracking in contrast to dry atmospheres. The cracking obviously exposes new metal to the oxidizer thus increasing the reaction rate. Numerous examples of this mechanism can be found in the literature (cf. Ref. 26).

NONISOTHERMAL EXPERIMENTS

Three sets of subignition experiments have been performed using the radiation of a carbon dioxide laser as heat source. The laser output was 110 watts, the exposure time 10 sec, and the atmospheres were water-pumped cylinder argon, lab air, and "aviator's breathing" oxygen. The sample holder was a graphite pan which was filled with Be powder approximately five particles deep.

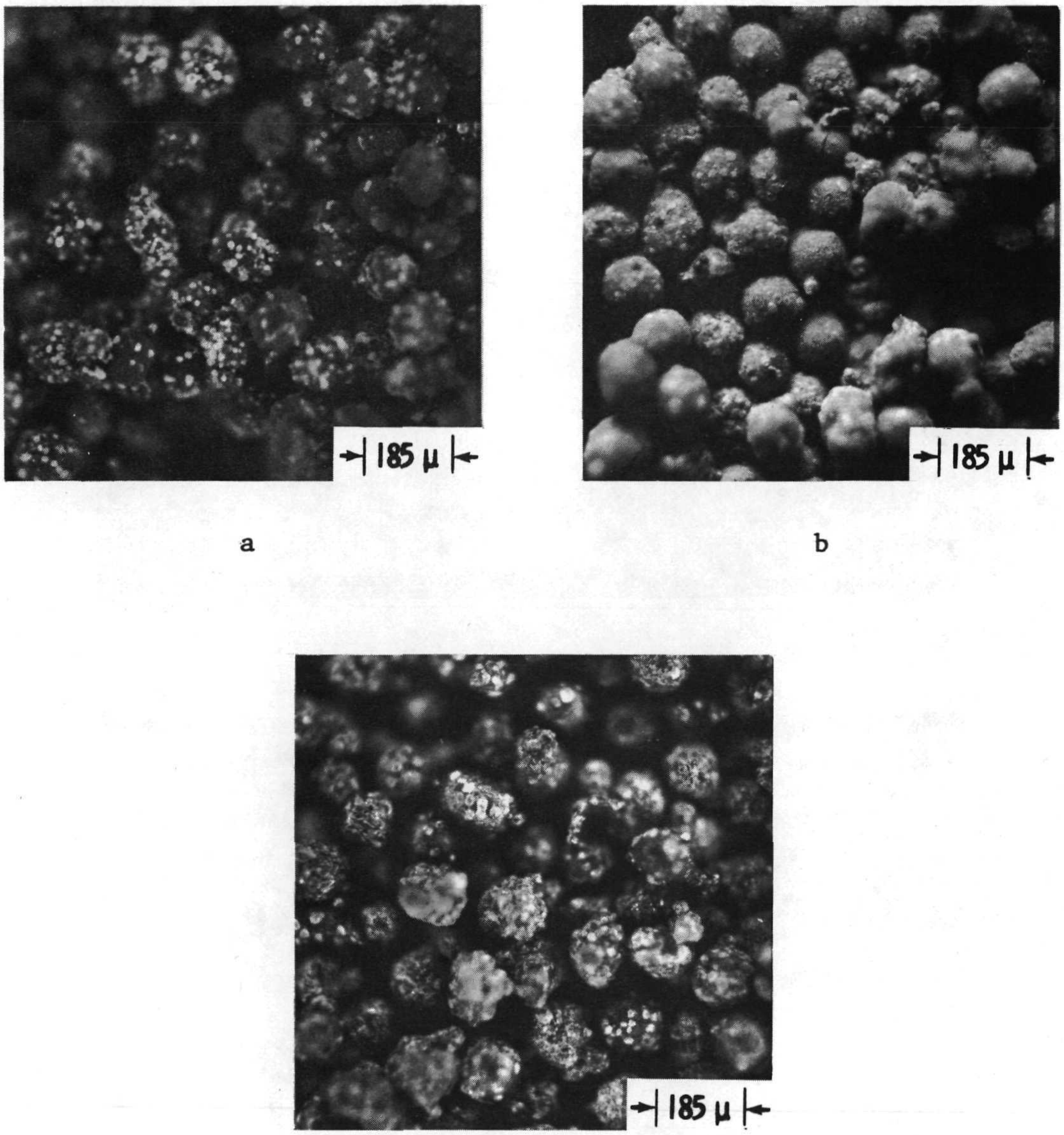

a

b

c

FIG. 5. Spherical Beryllium Particles After 8 Hours Heating (a) in Dry Argon, (b) Dry Nitrogen, and (c) Dry Oxygen. Heating temperature 900°C.

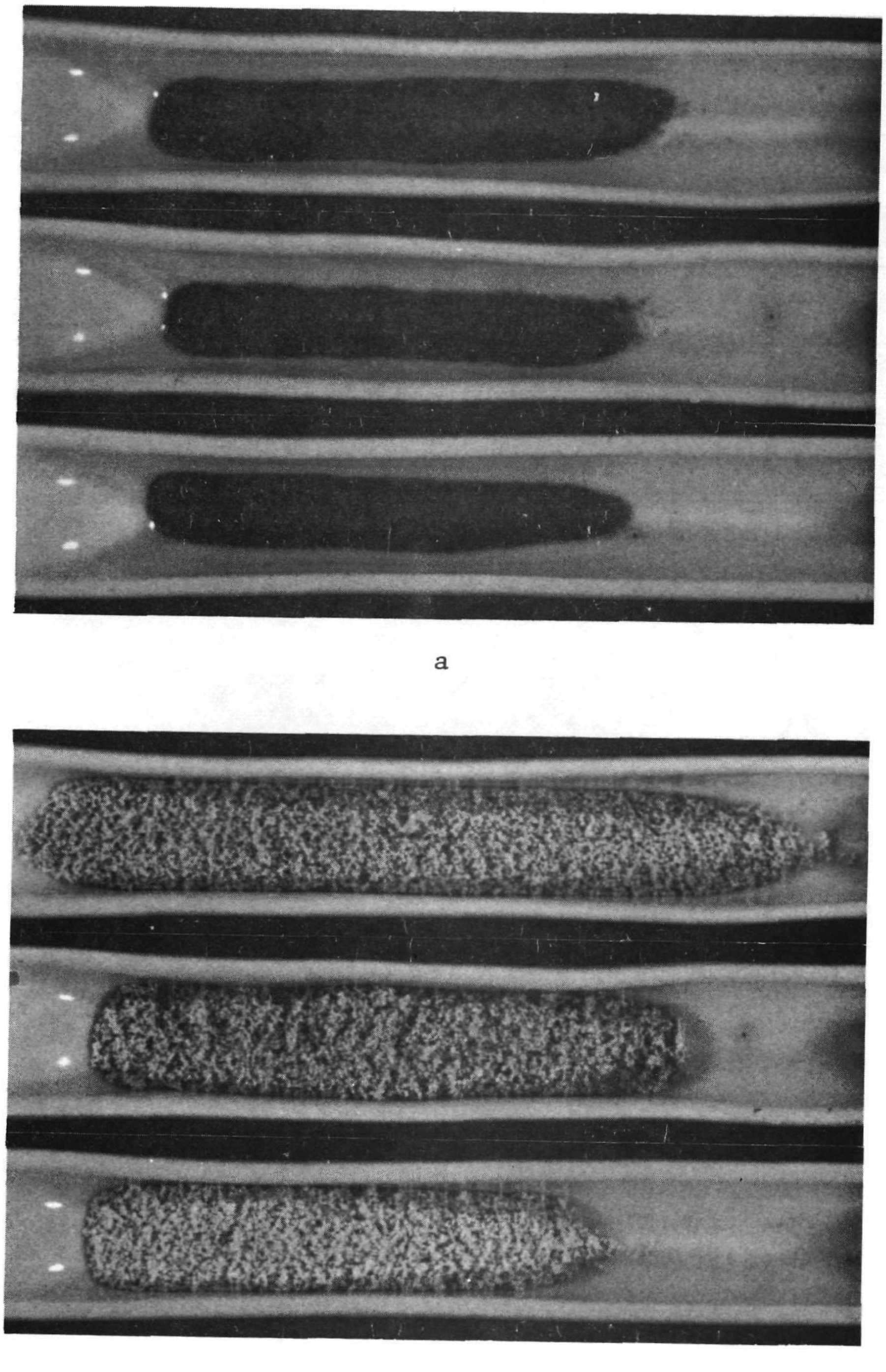

FIG. 6. Spherical Beryllium Particles (a) Before, and (b) After Heating (2 Hours at 900°C) in Moist Argon, Nitrogen, and Oxygen (from top to bottom).

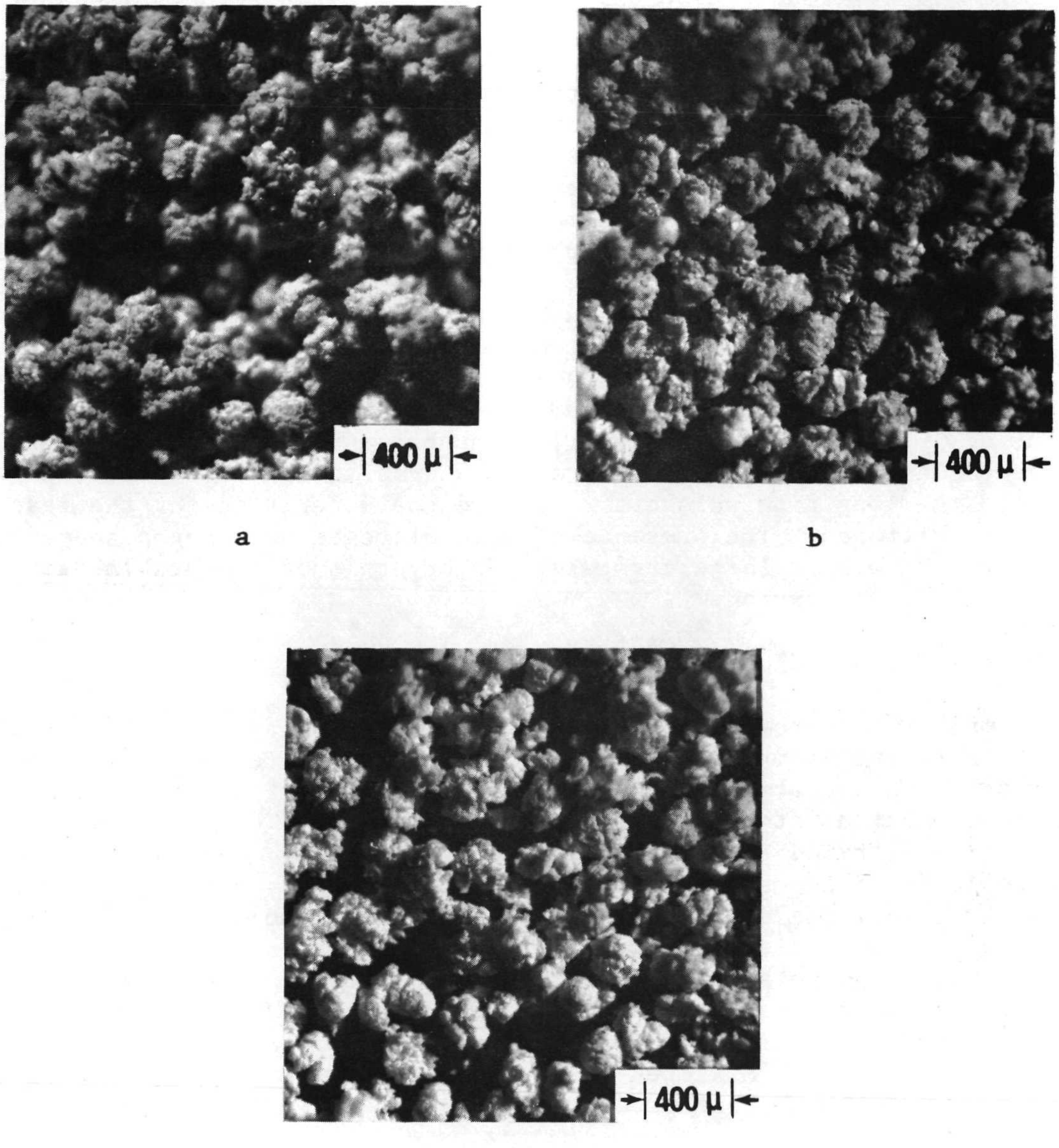

a

b

c

FIG. 7. Details of Beryllium Samples (see Fig. 6b) (a) After Heating in Moist Argon, (b) Moist Nitrogen, and (c) Moist Oxygen.

Very little reaction occurred during heating in argon. The surface of the particles became coarser and some of them were covered with a large number of small droplets resembling warts. These droplets probably developed during melting of the metal. Some huge agglomerates were found, as expected. Figure 8 shows part of an agglomerate which is approximately six times the diameter of the original particles. No agglomerate of this kind was ever observed in reactive atmospheres like air, nitrogen or oxygen. In these atmospheres the individual particles form a loose aggregate without ever producing large molten blobs of material.

Laser heating of Be powder in 1 atm air caused severe reaction and the formation of numerous product crystals of varying size. Figure 9 shows the sample after laser irradiation in air. The largest crystals developed in the center of the samples where the maximum temperature occurred. In cooler areas bordering the hot center the reaction product appeared less crystalline and more granular although some particles exhibited the long fine whiskers which are characteristic for the reaction of Be in nitrogen. The presence of both nitrogen and oxygen seemed to favor the growth of large crystals. No crystals of comparable size were obtained in pure oxygen.

SUMMARY AND CONCLUSIONS

Samples of Be powder heated to 900°C in a flow system employing dried argon, nitrogen or oxygen exhibited similar surface structure. During exposure to moist atmospheres the oxide lost much of its protectivity and the reaction rate was dramatically increased. This is similar to a condition described in the literature as "breakaway" oxidation. When heated in inert atmospheres Be agglomerated severely and formed large metal globules. In dry reactive atmospheres agglomeration of a sort occurred but particle clusters were formed instead of the usual coalescence into large metal globules. Vigorous reaction in nitrogen, oxygen, or air was achieved as a result of laser heating. Ignition was achieved only in oxygen. Ignited samples tended to burn intermittently at constant laser output. Mixtures of nitrogen and oxygen favored the development of large hexagonal product crystals.

C-2

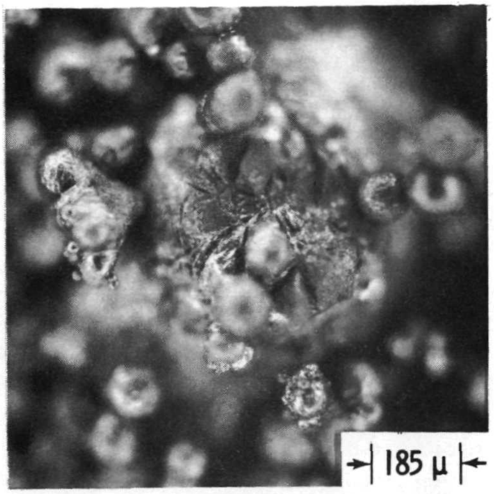

FIG. 8. Spherical Beryllium Particles After Exposure to Carbon Dioxide Laser Radiation in 1 atm of Argon. Laser output 110 watts, exposure time 10 sec.

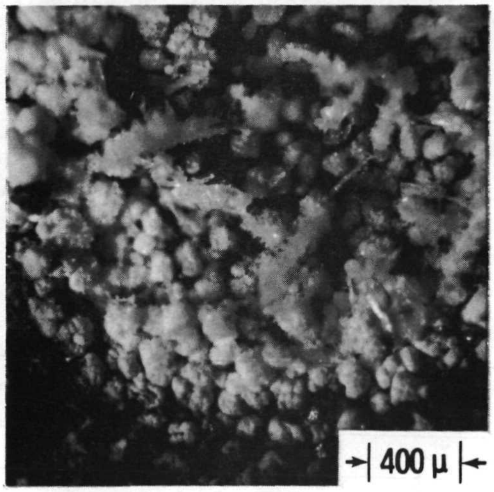

FIG. 9. Spherical Beryllium Particles After Exposure to Carbon Dioxide Laser Radiation in 1 atm of Air. Laser output 110 watts, exposure time 10 sec.

REFERENCES

1. Drew, C. M., A. S. Gordon and R. H. Knipe. *Study of Quenched Aluminum Particle Combustion, Progress in Astronautics and Aeronautics.* Ed. by H. G. Wolfhard, I. Glassman and L. Green, Jr. New York, Academic Press, 1964. Vol. 15, pp. 17-40.

2. Christensen, H. C., R. H. Knipe and A. S. Gordon. "Survey of Aluminum Particle Combustion," PYRODYNAMICS, Vol. 3, No. 1 and 2 (July 1965), pp. 91-119.

3. Drew, C. M. "Some Further Comments on the Paper, 'Estimating Aluminum Particle Combustion Kinetics,'" COMBUST AND FLAME, Vol. 9, No. 2 (June 1965), pp. 205-8.

4. Prentice, J. L., C. M. Drew and H. C. Christensen. "Preliminary Studies of High-Speed Photography of Aluminum Particle Combustion in Flames," PYRODYNAMICS, Vol. 3, No. 1 and 2 (July 1965), pp. 81-90.

5. Prentice, J. L. "On the Combustion of Single Aluminum Particles," COMBUST AND FLAME, Vol. 9, No. 2 (June 1965), pp. 208-10.

6. Drew, C. M., R. H. Knipe and A. S. Gordon. "The Morphology of Aluminum Particle Combustion," Meeting of the Western States Section/ The Combustion Institute, University of Denver, Denver, Colo., April 1966. Paper # WSS/CI 66-3.

7. U. S. Naval Ordnance Test Station. *Aluminum Particle Combustion Progress Report, 1 April 1964 - 30 June 1965*, by Metal Combustion Study Group. China Lake, Calif., NOTS, April 1966. 116 pp. (NOTS TP 3916).

8. Prentice, J. L. "Discussions on Heterogeneous Combustion," in *Eleventh Symposium (International) on Combustion.* University of California, Berkeley, Calif. The Combustion Institute, 1967. Pp. 215-17.

9. Gordon, A. S., C. M. Drew, J. L. Prentice and R. H. Knipe. "Techniques for the Study of the Combustion of Metals, A Review," AMER INST AERONAUT ASTRONAUT J, Vol. 6, No. 4 (April 1968), pp. 577-83.

10. Nelson, L. S., N. L. Richardson and J. L. Prentice. "Apparatus for the Production and Ignition of Metal Droplets with a Pulsed Laser," REV SCI INSTR, Vol. 39, No. 5 (May 1968), pp. 744-47.

11. Naval Weapons Center. *Metal Particle Combustion Progress Report, 1 July 1965 - 1 May 1967*, by Metal Combustion Study Group, edited by J. L. Prentice. China Lake, Calif., NWC, August 1968. 118 pp. (NWC TP 4435).

12. Prentice, J. L., and L. S. Nelson. "Differences Between the Combustion of Aluminum Droplets in Air and in an Oxygen-Argon Mixture," J ELECTROCHEM SOC, Vol. 115, No. 8 (August 1968), pp. 809-12.

13. Naval Weapons Center. *Metal Particle Combustion Progress Report, 1 May 1967 - 30 September 1968*, by J. L. Prentice and K. J. Kraeutle. China Lake, Calif., NWC,January 1969. 86 pp. (NWC TP 4658).

14. Boggs, T. L., J. L. Prentice, K. J. Kraeutle and J. E. Crump. "Role of the Scanning Electron Microscope in the Study of Solid Propellant Combustion," *Proceedings of the 2nd Annual Scanning Electron Microscope Symposium*. IIT Research Institute, Chicago, Ill., April 1969.

15. Crump, J. E., J. L. Prentice and K. J. Kraeutle. "Role of the Scanning Electron Microscope in the Study of Solid Propellant Combustion: II. Behavior of Metal Additives," COMBUSTION SCIENCE AND TECHNOLOGY, Vol. 1, No. 3 (November 1969), pp. 205-23.

16. Prentice, J. L. "Scanning Electron Microscopy of BeO Whiskers Formed on the Surface of Burning Beryllium Droplets," J AMER CERAM SOC, Vol. 52, No. 10 (October 1969),pp. 564-65.

17. ------. "Combustion of Pulse-Heated Single Particles of Aluminum and Beryllium," COMBUSTION SCIENCE AND TECHNOLOGY, Vol. 1, No. 5, (April 1970), pp. 385-98.

18. ------. "Effect of Water Vapor on the Combustion of Flash-Heated Beryllium Droplets," J ELECTROCHEM SOC, Vol. 117, No. 3 (March 1970), pp. 385-87.

19. ------. "Experimental Burning Rates of Single Laser-Ignited Beryllium Droplets," COMBUSTION SCIENCE AND TECHNOLOGY, Vol. 3, No. 6 (August 1971), pp. 287-94.

20. ------. "Reaction of Nitrogen with Burning Beryllium Droplets," COMBUSTION SCIENCE AND TECHNOLOGY, in press.

21. Macek, A. "Fundamentals of Combustion of Single Aluminum and Beryllium Particles," in *Eleventh Symposium (International) on Combustion*. University of California, Berkeley, Calif. The Combustion Institute, 1967. Pp. 203-14.

22. Nelson, L. S. "Nature of the Spearpoints Observed During the Combustion of Zirconium Droplets," NATURE, Vol. 207, No. 4998 (August 14, 1965), p. 741.

23. Macek, A. and J. McK. Semple. "Experimental Burning Rates and Combustion Mechanisms of Single Beryllium Particles," in *Twelfth Symposium (International) on Combustion.* Poitier, France. The Combustion Institute, 1969. Pp. 71-79.

24. Kuehl, D. K. and M. L. Zwillenberg. "Predictions of Burning Times of Metal Particles," *3rd ICRPG/AIAA Solid Propulsion Conference.* Atlantic City, New Jersey, June 4-6, 1968. Preprint No. 68-494.

25. Kirk, R. E. and D. F. Othmer, Editors. *Encyclopedia of Chemical Technology, 2nd Ed.* New York, John Wiley & Sons, Inc., 1967. Pp. 814-25.

26. Gulbransen, E. A. and K. J. Andrew. "The Kinetics of the Reactions of Beryllium with Oxygen and Nitrogen and the Effect of Oxide and Nitride Films on the Vapor Pressure," J ELECTROCHEM SOC, Vol. 97, No. 11 (November 1950), pp. 383-95.

27. Nelson, L. S. "Explosion of Zirconium Droplets Caused by Nitrogen," SCIENCE, Vol. 148, No. 3677 (18 June 1965), pp. 1594-95.

28. Gilles, J. C. "Formation of Oxynitrides from Refractory Oxides: A Study of Their Structures and Properties," REV HAUTE TEMPER ET REFRACT, Vol. 2, No. 3 (1965), pp. 237-62.

29. Orr, W. H. "Oxide Nucleation and Growth," Thesis, Cornell University, Microfilm, Inc., Ann Arbor, Michigan, ONR Rept. No. 5, April 1962.

30. Levine, H. S. "On the Initiation Mechanism for Explosion During Combustion of Metal Droplets," HIGH TEMPERATURE SCIENCE, Vol. 3, No. 3 (May 1971), pp. 237-43.

31. Nelson, L.S. "Combustion of Metal Droplets Ignited by Flash Heating," in *Eleventh Symposium (International) on Combustion.* University of California, Berkeley, Calif. The Combustion Institute, 1967. Pp. 409-15.

32. Meyer, R. T. and L. S. Nelson. "The Role of Nitrogen in the Formation of Microbubbles During the Explosive Combustion of Zirconium Droplets in N_2/O_2 Mixtures," HIGH TEMP SCIENCE, Vol. 2, No. 1 (March 1970), Pp. 35-57.

33. Meyer, R. T. and W. G. Breiland. "Nitrogen Thermochemistry During the Combustion of Zirconium Droplets in N_2/O_2 Mixtures," HIGH TEMP SCIENCE, in press.

INITIAL DISTRIBUTION

6 Naval Air Systems Command
  AIR-310 (1)
  AIR-330 (1)
  AIR-330B (1)
  AIR 5366A (1)
  AIR-604 (2)
2 Chief of Naval Material
  MAT-03L4 (1)
  NSP-27311, R. D. Kinert (1)
4 Naval Ordnance Systems Command
  ORD-033 (2)
  ORD-0632 (2)
2 Chief of Naval Research, Arlington
  ONR-102 (1)
  ONR-473, J. Patton (1)
1 Naval Ammunition Depot, Crane (Technical Library)
1 Naval Ordnance Laboratory, White Oak (Technical Library)
3 Naval Ordnance Station, Indian Head
  A. Camp (1)
  A. Roberts (1)
  Technical Library (1)
1 Naval Research Laboratory (Technical Library)
1 Naval Weapons Laboratory, Dahlgren (Technical Library)
1 Army Materiel Command (Robert Sehgal)
4 Army Missile Command, Redstone Arsenal
  B. J. Alley (1)
  Redstone Scientific Information Center, Chief Document Section (3)
2 Army Ballistics Research Laboratories, Aberdeen Proving Ground
  Interior Ballistics Laboratory, Dr. Ingo May (1)
  Technical Library (1)
1 Army Research Office, Durham (Technical Library)
2 Frankford Arsenal
  Martin Visnov (1)
  Technical Library (1)
2 Picatinny Arsenal
  C. Lenchitz (1)
  Technical Library (1)
1 Ogden Air Material Area, Hill Air Force Base (OOMOOP, Dr. Leonidas Brown)
2 Air Force Aeropropulsion Laboratory, Wright-Patterson Air Force Base
  Don Stull (1)
  Technical Library (1)

1 Air Force Office of Scientific Research (J. F. Masi)
2 Air Force Rocket Propulsion Laboratory, Edwards Air Force Base
  RPMCP, Dr. R. R. Weiss (1)
  Technical Library (1)
1 Armament Development & Test Center, Eglin Air Force Base (Technical Library)
1 Space and Missile Systems Organization, Norton Air Force Base (Technical Library)
1 Advanced Research Projects Agency (Technical Information Office)
12 Defense Documentation Center
1 Bureau of Mines, Pittsburgh (Explosive Research Center, I. Liebman)
3 Department of Transportation, Washington, D. C.
  Traffic Safety
    R. Cannon (1)
    W. Williams (1)
  FAA
    Patrick Russel (1)
6 National Aeronautics & Space Administration
  RP, W. Woodward (1)
  RPD, D. Hart (1)
  RPM, William Cohen (1)
  RPS, R. Wasel (1)
  ATSS-AC, Technical Library (2)
1 Ames Research Center (R&D Contracts Section, ASCR)
1 George C. Marshall Space Flight Center (Technical Library)
1 Goddard Space Flight Center (Technical Library)
4 Langley Research Center
  R. Levine (1)
  B. Northan (1)
  G. Pellet (1)
  Technical Library (1)
2 Lewis Research Center
  Dr. R. J. Priem (1)
  Technical Library (1)
2 Manned Spacecraft Center
  J. G. Thibodaux (1)
  Technical Library (1)
2 Aerojet Solid Propulsion Company, Sacramento, via AFPRO
  Head, Technical Information Office (1)
  P. Micheli (1)
1 Aerospace Corporation, Los Angeles, Calif. (Technical Library)
3 Allegany Ballistics Laboratory, Cumberland, Md.
  Hercules Representative, K. O. Hartman (1)
  Hercules Representative, R. Miller (1)
  Technical Library (1)
1 Applied Physics Laboratory, JHU, Silver Spring (Technical Library)
1 ARO, Incorporated, Arnold Air Force Station (N. S. Dougherty, Jr.)
3 Atlantic Research Corporation, Alexandria, Va.
  M. King (1)
  A. Macek (1)
  Technical Library (1)

DOCUMENT CONTROL DATA - R & D

(Security classification of title, body of abstract and indexing annotation must be entered when the overall report is classified)

1. ORIGINATING ACTIVITY *(Corporate author)* Naval Weapons Center China Lake, Calif. 93555	2a. REPORT SECURITY CLASSIFICATION UNCLASSIFIED 2b. GROUP

3. REPORT TITLE

Beryllium Particle Combustion (Final Report)

4. DESCRIPTIVE NOTES *(Type of report and inclusive dates)*

Final Report, 1 January 1969 to 31 December 1971

5. AUTHOR(S) *(First name, middle initial, last name)*

Jack L. Prentice

6. REPORT DATE	7a. TOTAL NO. OF PAGES	7b. NO. OF REFS
June 1972	62	33

8a. CONTRACT OR GRANT NO.	9a. ORIGINATOR'S REPORT NUMBER(S) NWC TP 5330
b. PROJECT NO. NASA Work Order No. 8201 c. d.	9b. OTHER REPORT NO(S) *(Any other numbers that may be assigned this report)*

10. DISTRIBUTION STATEMENT

Approved for public release; distribution unlimited.

11. SUPPLEMENTARY NOTES	12. SPONSORING MILITARY ACTIVITY National Aeronautics & Space Administration Ames Research Center Moffett Field, Calif. 94035

13. ABSTRACT

This report summarizes a two year study of the combustion efficiency of single beryllium droplets burning in a variety of oxidizers, but primarily mixtures of oxygen/argon and oxygen/nitrogen. An advanced laser heating technique has been used to acquire systematic quantitative data on the burning of single beryllium droplets at atmospheric pressure. This research confirms the sensitivity of beryllium droplet combustion to the chemistry of environmental species and provides experimental documentation for the nitrogen-induced droplet fragmentation of burning beryllium droplets. These studies clearly reveal the inadequacies of current droplet burning models as applied to beryllium but they also provide the sort of detailed, systematic foundation necessary for future rational development of the theory.

14. KEY WORDS	LINK A		LINK B		LINK C	
	ROLE	WT	ROLE	WT	ROLE	WT
Metal combustion						
Beryllium						
Single particles						
Laser ignition						

1 Bermite Division of Tasker Industries, Saugus, Calif. (Technical Library)
1 Brigham Young University, Provo, Utah (R. L. Coates)
2 Chemical Propulsion Information Agency, Applied Physics Laboratory, Silver Spring, Md.
  T. W. Christian, III (1)
  Technical Library (1)
1 California Institute of Technology, Pasadena, Calif. (F. E. C. Culick)
1 Factory Mutual Research Corporation, Norwood, Mass. (Dr. G. H. Markstein)
1 Georgia Institute of Technology, Atlanta, Ga. (School of Aerospace Engineering, Dr. W. Strahle)
2 Hercules, Inc., Bacchus Works, Magna, Utah
  Dr. M. W. Beckstead (1)
  Technical Library (1)
1 Institute for Defense Analyses, Arlington (Technical Library)
7 Jet Propulsion Laboratory, CIT, Pasadena, Calif.
  Warren Dowler (6)
  Technical Library (1)
2 Lockheed Missiles & Space Company, Palo Alto, Calif.
  O. Krone (1)
  C. A. Zimmerman (1)
2 Lockheed Propulsion Company, Redlands, Calif.
  Dr. R. L. Derr (1)
  Technical Library (1)
3 Princeton University, Forrestal Campus Library, Princeton, N. J.
  Dr. Irvin Glassman (1)
  Dr. Martin Summerfield (1)
  Technical Library (1)
3 Purdue University, Lafayette, Ind.
  A. M. Mellor (1)
  J. R. Osborn (1)
  Technical Library (1)
2 Rocketdyne, Canoga Park, Calif.
  J. E. Flanagan (1)
  Technical Library (1)
2 Rocketdyne, McGregor, Tex.
  W. Haymes (1)
  Technical Library (1)
4 Sandia Corporation, Albuquerque, N. M.
  Dr. Lloyd S. Nelson (1)
  H. S. Levine (1)
  R. T. Meyer (1)
  Technical Library (1)
1 Science & Technology Information Facility, Bethesda, Md. (CRT)
1 Stanford Research Institute, Menlo Park, Calif. (Technical Library)
1 Stevens Institute of Technology, Hoboken, N. J. (Mechanical Engineering Department, R. F. McAlevy III)
1 Thiokol Chemical Corporation, Elkton, Md. (Technical Library)
2 Thiokol Chemical Corporation, Huntsville Division, Huntsville, Ala.
  D. A. Flanigan (1)
  Technical Library (1)

2 Thiokol Chemical Corporation, Wasatch Division, Brigham City, Utah
    G. Petersen (1)
    Technical Library (1)
1 TRW Systems, Redondo Beach, Calif. (Technical Library)
1 United Aircraft Corporation, East Hartford, Conn. (Research Laboratories, R. H. W. Waesche)
2 United Technology Center, Sunnyvale, Calif.
    Dr. R. S. Brown (1)
    Technical Library (1)
1 University of California, Berkeley, Calif. (Chemistry Department, E. Peterson)
1 University of California, San Diego, La Jolla, Calif. (Prof. F. A. Williams)
2 University of Denver, Denver Research Institute, Denver, Colo.
    W. McLain (1)
    R. Williams (1)
2 University of Utah, Salt Lake City, Utah
    Prof. A. Baer (1)
    Prof. N. W. Ryan (1)
1 Yale University, New Haven, Conn. (Prof. Daniel Rosner)